

# Himalayan leucogranites and migmatites: nature, timing and duration of anatexis

R. F. WEINBERG

School of Earth, Atmosphere and Environment, Monash University, Clayton, Vic. 3800, Australia  
(roberto.weinberg@monash.edu)

**ABSTRACT** Widespread anatexis was a regional response to the evolution of the Himalayan-Tibetan Orogen that occurred some 30 Ma after collision between Asia and India. This paper reviews the nature, timing, duration and conditions of anatexis and leucogranite formation in the Greater Himalayan Sequence (GHS), and compares them to contemporaneous granites in the Karakoram mountains. Himalayan leucogranites and associated migmatites generally share a number of features along the length of the mountain front, such as similar timing and duration of magmatism, common source rocks and clockwise  $P$ – $T$  paths. Despite commonalities, most papers emphasize deviations from this general pattern, indicating a fine-tuned local response to the dominant evolution. There are significant differences in  $P$ – $T$ – $X_{\text{H}_2\text{O}}$  conditions during anatexis, and timing in relation to regional decompression. Further to that, some regions underwent a second event recording melting at low pressures. Zircon and monazite ages of anatectic rocks range between *c.* 25 and 15 Ma, suggesting prolonged crustal melting. Typically, a single sample may have ages covering most of this 10 Ma period, suggesting recycling of accessory phases from metamorphic rocks and early-formed magmas. Recent studies linking monazite and zircon ages with their composition, have determined the timing of prograde melting and retrograde melt crystallization, thus constraining the duration of the anatectic cycle. In some areas, this cycle becomes younger down section, towards the leading front of the Himalayas, whereas the opposite is true in other areas. The relationship between granites and movement on the South Tibetan Detachment (STD) reveals that fault motion took place at different times and over different durations requiring complex internal strain distribution along the Himalayas. The nature and fate of magmas in the GHS contrast with those in the Karakoram mountains. GHS leucogranites have a strong crustal isotopic signature and migration is controlled by low-angle foliation, leading to diffuse injection complexes concentrated below the STD. In contrast, the steep attitude of the Karakoram shear zone focused magma transfer, feeding the large Karakoram-Baltoro batholith. Anatexis in the Karakoram involved a Cretaceous calcalkaline batholith that provided leucogranites with more juvenile isotopic signatures. The impact of melting on the evolution of the Himalayas has been widely debated. Melting has been used to explain subsequent decompression, or conversely, decompression has been used to explain melting. Weakening due to melting has also been used to support channel flow models for extrusion of the GHS, or alternatively, to suggest it triggered a change in its critical taper. In view of the variable nature of anatexis and of motion on the STD, it is likely that anatexis had only a second-order effect in modulating strain distribution, with little effect on the general history of deformation. Thus, despite all kinds of local differences, strain distribution over time was such that it maintained the well-defined arc that characterizes this orogen. This was likely the result of a self-organized forward motion of the arc, controlled by the imposed convergence history and energy conservation, balancing accumulation of potential energy and dissipation, independent of the presence or absence of melt.

**Key words:** anatexis; continental collision; leucogranite; migmatite; self-organization.

## INTRODUCTION

Miocene granites and migmatites are some of the most studied features of the Himalayan-Tibetan Orogen. They are central to understanding its evolution and the basis for many evolutionary models (England *et al.*, 1992; Harris & Massey, 1994; Huerta *et al.*, 1996; Harrison *et al.*, 1997a, 1998, 1999b; Hodges,

1998). Decades of research helped elucidate their spatial distribution, timing and conditions of anatexis, as well as their role in the evolution of the Orogen. Yet their relative timing in relation to major structures, the origin of the heat source for melting and the tectonic impact of melting, remain widely debated (Hodges, 2000; Yin & Harrison, 2000; Kohn, 2014). Several tectonic models have been presented to

explain the evolution of these mountains (see Kohn, 2014 for a summary) many of which are fundamentally linked to crustal melting. For example, channel models require the presence of melt, weakening thick sections of the Greater Himalayan Sequence (GHS), to allow the flow of rocks from underneath Tibet (Beaumont *et al.*, 2001; Grujic *et al.*, 2002; Jamieson *et al.*, 2004).

Miocene granitoids are typically Ms–Bt–Grt–Tur peraluminous leucogranites, and crop out in three distinct regions in the Orogen with significant tectono-thermal and temporal differences: (i) within the GHS along the Himalayan front, cropping out between the Main Central Thrust (MCT) zone and the South Tibetan Detachment (STD), and known as Greater or Higher Himalayan leucogranites; (ii) north of the STD, in association with domes (the North Himalayan granites; Le Fort, 1986; Harrison *et al.*, 1998; King *et al.*, 2011); and (iii) in the Karakoram Range, north of the Indus-Tsangpo Suture Zone (Fig. 1). A fourth and much younger anatectic event (<4 Ma) is exposed in the two syntaxes, at Namche Barwa and Nanga Parbat.

This article reviews the literature on migmatites and leucogranites (referred to collectively as anatectic rocks) of the GHS and then contrasts them to anatectic rocks from the Karakoram Range. The focus is dominantly on the more recent literature

and key features significant to understanding the origin of collisional granitoids and the behaviour of the Orogen. It is demonstrated how the process of granite generation is simultaneously tightly constrained as well as highly variable responding to local conditions. The paper starts with an introduction to the geological setting of the anatectic rocks, followed by: (i) melting conditions and melting reactions across the Orogen; (ii) timing and duration of magmatism, and significance for granite generation; and (iii) granite ages constraining movement duration on the STD. The section on melting conditions (i) is separated from the section on timing and duration of magmatism (ii) in order to emphasize changing patterns along the Himalayas. Himalayan anatectic rocks are then contrasted to those from the Karakoram before a discussion focusing on how the data inform and constrain the tectonic evolution of the Orogen. The paper finishes by suggesting that the variety of conditions and timing of magma generation and movement on the STD had only a second-order effect in modulating strain distribution. These were local responses to a broader pattern of self-organized motion imposed by the potential energy stored in the Orogen and the continued northward indentation of India, which allowed for the orderly development of the Orogen and maintenance of the orogenic arc.

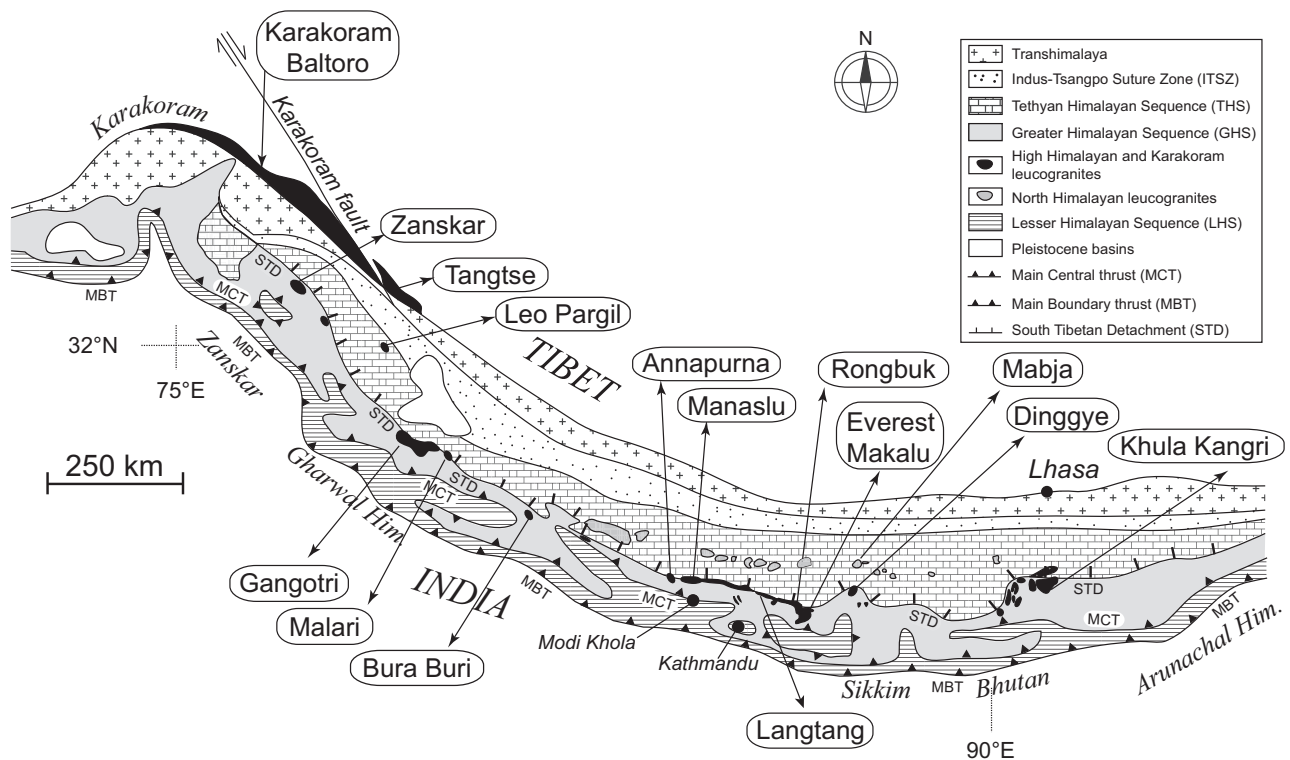


**Fig. 1.** Simplified geological map of the southern part of the Himalayan-Tibet Orogen showing the GHS, between the STD and the MCT, and the two belts of leucogranites, including the Karakoram-Baltoro Batholith on the upper left (NW) of the figure. Locations refer to those mentioned in the text.

## GEOLOGICAL SETTING OF LEUCOGRANITES

The Himalayas and the Tibetan plateau result from collision between India and Asia between 54 and 50 Ma (Hodges, 2000). The Himalayas form a well-defined arc, with a sinuous front forming salients and recesses at the scale of a few 100 km in length (Bendick & Bilham, 2001; Mukul, 2010). Hodges (2000), building on previous work, divided the evolution of the Himalayas into two deformation phases, linked to distinct metamorphic events: the Middle Eocene–Late Oligocene Eohimalayan, recording crustal thickening with metamorphism peaking at *c.* 33–28 Ma; and the Early Miocene to present Neohimalayan phase, associated with sillimanite-bearing rocks, anatexis and leucogranite intrusions. This phase is associated with a substantial change in tectonics at the start of the Miocene, and remains roughly unchanged, suggesting a quasi-steady-state orogenic system (Hodges, 2000).

The Himalayas are divided into three main sequences: the Lesser, Greater and Tethyan Himalayan Sequences (LHS, GHS and THS, respectively, following Kohn's 2014 terminology). The GHS is a high-grade package sandwiched between greenschist facies metasedimentary rocks of the LHS below and THS above. The MCT separates the GHS from the underlying LHS, and the STD separates the GHS from the overlying THS. The GHS varies in thickness from 3 to 5 km (Vannay & Hodges, 1996; Carosi *et al.*, 2007) to ~20 km in Bhutan (Grujic *et al.*, 1996) to 25–30 km thick in the Makalu region (Streule *et al.*, 2010; see also Goscombe *et al.*, 2006). Himalayan stratigraphy, the main structural features and metamorphic grade are all reasonably consistent along strike for 2000 km (Hodges, 2000). There is typically a sharp and continuous upward increase in temperature and pressure across the MCT, giving rise to an inverted metamorphic gradient (summarized in Harrison, 2006; Kohn, 2014) so that peak temperatures rise to 700–800 °C across the MCT, recorded by muscovite-dehydration melting reactions (Kohn, 2014), and in some places biotite-dehydration melting reactions (e.g. Groppo *et al.*, 2010b; Rubatto *et al.*, 2013). Anatexis is recorded by stromatic migmatite sequences, reaching 10 km in structural thickness that feed sills (Searle, 2013). The MCT has complex and varied local histories (Larson *et al.*, 2015), having been established as early as 23–20 Ma (Hubbard & Harrison, 1989; Hodges *et al.*, 1996) and active as late as in Late Miocene–Pliocene times (Harrison *et al.*, 1997b; Catlos *et al.*, 2004).

The STD is a complex structure generally defined by a wide ductile normal shear zone, at times overprinted by younger, brittle normal faults (e.g. Kellett & Grujic, 2012). It acts as a decoupling horizon that either telescopes or truncates the metamorphic sequence in the upper parts of the GHS (e.g. Burg & Chen, 1984; Burg *et al.*, 1984; Dèzes *et al.*, 1999) and

separates it from the low-metamorphic grade rocks of the THS. It began moving prior to 22 Ma, and has had a short duration in some places (Hodges *et al.*, 1996; Carosi *et al.*, 2013; Finch *et al.*, 2014), whereas in others it may have continued to move to *c.* 11 Ma (Kellett *et al.*, 2009).

Miocene migmatites are found from within the MCT zone (Hubbard, 1989; Coleman, 1998; Dasgupta *et al.*, 2009) to the base of the STD (Pognante, 1992; Kohn, 2014). Migmatites are commonly, but not solely, developed in the 500–400 Ma gneisses at the top of the GHS (e.g. Sikkim, Dasgupta *et al.*, 2009; Zanskar, Finch *et al.*, 2014; Horton *et al.*, 2015; E Nepal, Groppo *et al.*, 2012). These are physically linked with granites through complex channel networks. The Higher Himalayan leucogranites form a discontinuous belt along the highest structural levels of the GHS, generally immediately below or overprinted by the STD. The belt extends for nearly 3000 km along strike of the High Himalayas from northern Pakistan to Bhutan (e.g. Harris *et al.*, 1993). The total volume of leucogranite intrusions is small (Le Fort, 1986; Harrison, 2006) and the larger accumulations result from a network of sheets, sills and dykes, exploiting foliation anisotropy (Scaillet *et al.*, 1996; Weinberg & Searle, 1999; Finch *et al.*, 2014) and emplaced at temperatures of ~700–750 °C. Although in some areas granites intrude the base of the Tethyan Himalayan Series (summary in Hodges, 2000), the accumulation of magma within and beneath the STD suggest that the steep temperature gradient imposed by normal movement acted as a powerful barrier to magma migration (Finch *et al.*, 2014).

## REGIONAL MELTING – LOCAL CONDITIONS

Himalayan leucogranites vary in age from 25 to 15 Ma (Leech, 2008), with the largest plutons formed at *c.* 21 ± 1 Ma (Harrison, 2006). Leucogranites vary in modal proportions of mica, garnet and tourmaline, and occasionally have cordierite, andalusite or sillimanite (e.g. Visonà *et al.*, 2012). There have been attempts to determine systematic temporal variations of leucogranite chemistry and mineralogy (Guillot & Le Fort, 1995). While there may be clear patterns in some areas (e.g. Patiño Douce & Harris, 1998), in other areas there are multiple cross-cutting relationships of granites with different mineralogy showing little systematics, or conversely, similar granites but with a 4 Ma age difference between them (Coleman, 1998, p. 569). There is also a range of migmatite types with different paragenesis, typically with sillimanite, in some cases garnet (e.g. Ferrero *et al.*, 2012; Groppo *et al.*, 2012; Rubatto *et al.*, 2013), cordierite and andalusite in the uppermost GHS (Streule *et al.*, 2010; Visonà *et al.*, 2012; Groppo *et al.*, 2013), or kyanite, this typically found close to or within the MCT (Coleman, 1998; Daniel *et al.*, 2003; Iaccarino *et al.*, 2015). Other migmatites lack

anhydrous peritectic minerals altogether (Finch *et al.*, 2014). Evidence for an Eohimalayan melting event has been found in the form of nanotonalites inclusions in garnet in kyanite-bearing gneisses and dated indirectly to have formed at 41–36 Ma (Carosi *et al.*, 2015).

Anatexis of the GHS may have been a regional event, but melting conditions and melting reactions were variable and responded to local conditions, as indicated by variable peritectic minerals, suggesting different metamorphic histories (Table 1). As summarized by Hodges (2000), there has been considerable controversy regarding the role of fluids in the origin of Himalayan granites. Le Fort *et al.* (1987), summarizing previous work in Nepal, suggested that Himalayan leucogranites resulted from thrusting along the MCT, during which large quantities of fluids were liberated below and fluxed the hotter upper slab causing anatexis (Fig. 2). This hypothesis was subsequently rejected by Harris and collaborators, who investigated the behaviour of Rb, Sr, Ba in leucogranites and found that 'isotope systematics and metamorphic phase equilibria have identified micaceous metasedimentary rocks as the most likely source, and the incongruent melting of muscovite as the appropriate melting reaction' (Harris *et al.*, 1993). More recently, Guo & Wilson (2012) found that fluids released from the LHS metasomatized the GHS before decompression and melting.

The prevalence of clockwise  $P$ – $T$  paths recorded by Himalayan metamorphic rocks (e.g. Pecher, 1989) led Harris & Massey (1994) to conclude that most Himalayan granites resulted from decompression melting within the sillimanite field, between 9 and 4 kbar and 650 and 750 °C. Using muscovite schists and biotite–muscovite schists from the GHS, Patiño Douce & Harris (1998) generated leucogranite melts similar to Himalayan leucogranites at 6–8 kbar and 750–770 °C, the likely conditions for Himalayan metamorphism (Scaillet *et al.*, 1995b). The dominant view in the literature, strongly shaped by these works, has been that rapid decompression of hot rocks has led to melting, generally as a result of muscovite dehydration (see discussions in Harris *et al.*, 1995; Harrison *et al.*, 1999a; Knesel & Davidson, 2002). More recent works, however, show varied conditions and melting histories at a range of  $P$ – $T$ – $X_{\text{H}_2\text{O}}$  conditions (Table 1), varying from water-fluxed melting (e.g. Badrinath, Prince *et al.*, 2001; Zanskar, Finch *et al.*, 2014), to biotite-dehydration melting (e.g. Sikkim, Dasgupta *et al.*, 2009; Rubatto *et al.*, 2013, and central-east Himalaya Visonà *et al.*, 2012). In some cases, melting reactions evolved from muscovite to biotite dehydration (e.g. Sikkim, Rubatto *et al.*, 2013), or from dehydration melting to water-fluxed melting (Zanskar, Pognante & Lombardo, 1989; Finch *et al.*, 2014). In other cases there were two separate and distinct melting events (Streule *et al.*, 2010), or melting occurred as a result of heating and decompression at relatively low pressures

(Streule *et al.*, 2010; Groppo *et al.*, 2012) or of heating at low pressure (Visonà & Lombardo, 2002; Streule *et al.*, 2010; Groppo *et al.*, 2012, 2013; Visonà *et al.*, 2012).

The article follows the terminology of Weinberg & Hasalová (2015) and refers to water-fluxed melting for melting in the presence of a  $\text{H}_2\text{O}$ -rich phase, also known as water-present melting or wet melting. Muscovite- and biotite-dehydration melting reactions refer to anatexis triggered by the breakdown of the two hydrate phases, in the absence of an aqueous phase (vapour-absent melting reactions). Note that water-fluxed melting does not necessarily produce  $\text{H}_2\text{O}$ -saturated melts. Like dehydration melting, water-fluxed melting can produce undersaturated melts and stabilize anhydrous peritectic minerals (Weinberg & Hasalová, 2015). All examples presented are summarized in Table 1.

### Water-fluxed melting

#### *Alakhnanda-Saraswati valleys: Garhwal Himalayas*

The two mica, garnet leucogranites exposed in this region are possibly the oldest record of melting in the Himalayas, and are associated with the presence of aqueous fluids (Prince *et al.*, 2001). Garnet in leucogranite was dated by Sm–Nd and yielded an age of  $39 \pm 5$  Ma, some 15 Ma before the main Himalayan anatexis, and contrasting with the  $19 \pm 0.5$  Ma by U–Pb zircon age (LA-ICP-MS) of the Malari granite immediately to the east (Sachan *et al.*, 2010). Prince *et al.* (2001) estimated melting conditions at  $720 \pm 40$  °C and  $7 \pm 2$  kbar, from which they concluded that melting was water-fluxed (Fig. 3a), which may have caused rapid melting and melt extraction, leading to disequilibrium, explaining the high Eu anomaly and unusually low Rb/Sr ratios of these rocks.

These rocks are in the vicinity of the Badrinath and *c.* 20 Ma Gangotri Tur + Ms ± Bt leucogranites, which combine to form one of the largest granite bodies in the GHS (Scaillet *et al.*, 1990). The melting reaction that originated these leucogranites is undetermined, but Rb/Sr isotope data are heterogeneous suggesting that they are comprised of batches from different isotopic sources and not subsequently homogenized. The O isotopes suggest a source with homogeneous O-isotope signature, interpreted to be a result of an earlier fluid infiltration (Scaillet *et al.*, 1990), in contrast to the heterogeneous O-isotope values of the Manaslu granite, Nepal (Deniel *et al.*, 1987).

### Dehydration melting overprinted by water-fluxed melting

#### *Zanskar*

In the Zanskar range, the *c.* 500–400 Ma Kade orthogneiss and metapelites of the GHS form

**Table 1.** Summary of anatexis in the GHS divided by melting reaction and by location. Table includes Karakoram Shear Zone.

Location	Leucogranite/ leucosome mineralogy	Age range (method)	<i>P-T</i> estimates	<i>P-T</i> history	References
<b>Water-fluxed melting</b>					
Alakhnanda-Saraswati valleys, Garhwal Himalayas	Two-mica, garnet leucogranites	39 ± 5 Ma (Grt Sm–Nd). Main melting: 19 ± 0.5 Ma (U–Pb zircon)	720 ± 40 °C 7 ± 2 kbar	Disequilibrium melting due to water influx	Prince <i>et al.</i> (2001); Sachan <i>et al.</i> (2010)
Badrinath and Gangotri, Garhwal Himalayas	Tur–Ms–Bt leucogranites	21.1 ± 0.9 Ma (Rb–Sr mineral isochron, WR, Tur, two Fsp, Ms). 18.9 ± 1.3 Ma (K–Ar Ms separate)	Not available	Fluid infiltration in the source predating peak <i>P-T</i> leading to homogenous O-isotope signature	Stern <i>et al.</i> (1989); Scaillet <i>et al.</i> (1990)
Karakoram Shear Zone, Ladakh	Two-mica–Grt–Tur leucogranites, Hbl-leucogranite	26–13 Ma (U–Pb zircon and monazite)	700–750 °C 4–5 kbar	Synkinematic melting in Shear Zone by influx of water. Two rock sources: biotite-rich clastic sequence and 100–60 Ma calc-alkaline granitoids	Rolland & Pêcher (2001); Reichardt <i>et al.</i> (2010); Boutonnet <i>et al.</i> (2012); Reichardt and Weinberg (2012a,b) see main text for full list
<b>Dehydration melting overprinted by water-fluxed melting</b>					
Zaskar	Two-mica–Grt–Tur leucogranites	26.6–19.8 Ma (U–Th–Pb monazite, SIMS, ID-TIMS)	650–720 °C 4–7 kbar 800 °C 8 kbar	Initial Ms- and Bt-dehydration as a result of decompression from 10 to 6 kbar. Subsequent water-fluxed melting. Continuous anatexis across switch from reverse to normal movement	Pognante (1992); Massey <i>et al.</i> (1994); Vance & Harris (1999); Robyr <i>et al.</i> (2006); Finch <i>et al.</i> (2014); Horton <i>et al.</i> (2015)
Manaslu	Two-mica–Tur leucogranites	Two melting events: 22.9 ± 0.6 Ma 19.3 ± 0.3 Ma (Th–U monazite)		Ms-dehydration melting producing low-Sr magma, followed by water-fluxed melting and high-Sr magma	Harrison <i>et al.</i> (1999a,b); Knesel & Davidson (2002)
<b>Ms-dehydration melting</b>					
Langtang	Ms ± Tur/Bt	20–17 Ma	710–760 ± 30 °C 10–5.8 ± 0.4 kbar	Heating and melting preceding or during decompression. Disequilibrium in source – fast melt extraction	Inger & Harris (1992); Harris <i>et al.</i> (1993); Harris & Massey (1994)
Makalu granites and migmatites (structurally shallow parts of the GHS)	Low- <i>P</i> cordierite-bearing leucogranites possibly sourced from Barun gneiss intrude older Grt–Tur–Ms ± Bt leucogranites. See also And-leucogranite below	Metam. <i>c.</i> 35–30 Ma. Main leucogranite: 24–21 Ma (Zrc–Mnz). Crd-bearing granite protracted melting: 19–16 Ma (U–Pb, Mnz–Xtm, LA-MC-ICP-MS)	Peak muscovite-dehydration melting at 713 °C – 5.9 kbar followed decompression reaching the solidus at ~600 °C – 2 kbar	Heating followed by decompression within the field of muscovite dehydration melting	Streule <i>et al.</i> (2010); Groppo <i>et al.</i> (2013)
<b>Ms-dehydration evolving into Bt-dehydration melting</b>					
Eastern Nepal – MCT at Arun Tectonic Window. Dominantly Ms-dehydration melting and incipient Bt-dehydration	Grt–Ky anatectic gneisses at highest levels of MCT	31.0 ± 0.4 Ma (U–Pb, Pb–Pb Mnz, SHRIMP)	Peak conditions: 820 °C, 13 kbar. Decompression: 805 °C, 10 kbar. Alternative peak conditions: >790 °C – 10.5 kbar	Clockwise <i>P-T</i> , melting predating decompression during prograde path in stability field of kyanite	Groppo <i>et al.</i> (2010); Groppo <i>et al.</i> (2009)
Sikkim and E Nepal. Progression from water-fluxed to Ms- and Bt-dehydration melting	Leucosomes: Sil ± Bt ± Grt	Anatexis from 31 to 17 Ma. Peak conditions at higher structural levels 26–21 Ma, and at lower levels 31–27 Ma (U–Pb, Mnz–Zrc, SHRIMP): 33–16 Ma in E Nepal	800 °C 8–10 kbar decompression to 5 kbar	Melting during heating from ~700 °C (prograde path), followed by rapid decompression at <i>c.</i> 25 Ma due to melting, lasting a few millions years	Harris <i>et al.</i> (1993); Ganguly <i>et al.</i> (2000); Dasgupta <i>et al.</i> (2009); Kellett <i>et al.</i> (2009); Imayama <i>et al.</i> (2012); Rubatto <i>et al.</i> (2013); Sorcar <i>et al.</i> (2014); Gaidies <i>et al.</i> (2015)
<b>Bt-dehydration melting</b>					
Makalu area, Barun gneisses (structurally deep within the GHS)	Grt + Sil + Ky stromatic migmatites		800–850 °C 8–10 kbar decompression to 7 kbar	Clockwise <i>P-T</i> path, melting prior to decompression	Groppo <i>et al.</i> (2012)
Everest to Kangchenjunga migmatites	Low- <i>P</i> cordierite-bearing migmatite, possible source of andalusite granites		750–800 °C 4–6 kbar	Melting due to low- <i>P</i> isobaric prograde heating	Groppo <i>et al.</i> (2013)

**Table 1.** (Continued)

Location	Leucogranite/ leucosome mineralogy	Age range (method)	<i>P-T</i> estimates	<i>P-T</i> history	References
Everest to Bhutan	Low- <i>P</i> andalusite leucogranites: several phases of andalusite from residual/peritectic early magmatic to late magmatic (And + Ms + Bt ± Crd ± Sil ± Sp ± Ky ± Crn)	15.9 ± 0.4 Ma (U-Pb zircon) overprinting an earlier (24–21 Ma) melting event	660–700 °C <4 kbar	Two melting events: (i) Predating and synchronous with decompression, and (ii) isobaric heating at low pressure (<4 kbar)	Visonà & Lombardo (2002); Kellett <i>et al.</i> (2009); Visonà <i>et al.</i> (2012)

migmatites that are linked to leucogranites. These accumulate as sills and dykes at the top of the GHS (Pognante & Lombardo, 1989; Pognante, 1992; Dèzes *et al.*, 1999; Walker *et al.*, 1999; Finch *et al.*, 2014) forming an injection complex within the Zanskar Shear Zone, the local name for the STD (Fig. 3b). The shear zone and migmatites are separated by a gneiss band intruded by sills and dykes 1–2 km thick (Finch *et al.*, 2014).

Anatexis started with muscovite-dehydration melting at 650–720 °C and 4–7 kbar, as a result of decompression, followed by extensive melting due to water-fluxing (Pognante, 1992), accounting for the large melt fraction (Fig. 3c,d). Vance & Harris (1999) found that garnet in Zanskar grew between 35 and 25 Ma, during prograde heating to 700 °C and a pressure increase from 6 to 10 kbar. They suggested subsequent rapid decompression by at least 4 kbar triggered muscovite-dehydration melting. Harris & Massey (1994) also linked melting to rapid decompression and normal movement on the STD, but this is most unlikely given that anatexis had already started during thrusting (Finch *et al.*, 2014).

A recent study of migmatitic paragneisses from the core of the migmatite terrane yielded 800 °C and 8 kbar (Robyr *et al.*, 2006) suggesting biotite-dehydration melting could have occurred. This is

consistent with our own observations, where biotite-dehydration melting is indicated by regions where the volume of leucosome is small and garnet is preserved in leucosomes (Fig. 3c). The subsequent water-fluxed melting, argued by Pognante (1992) led to the destabilization of garnet, thus erasing much of the evidence for early dehydration melting in most places, and explaining the general lack of anhydrous peritectic minerals in regions with voluminous leucosomes (Fig. 3d). Finch *et al.* (2014) suggested that the syn-anatectic switch from reverse to normal movement in Zanskar could have been a result of fluid influx and extensive melting, destabilizing the taper angle.

#### Manaslu

The Manaslu intrusive complex is one of the type-localities for Himalayan leucogranites. The isotopic composition of the complex has been the focus of much interest since the work of Deniel *et al.* (1987) who showed large isotopic variation even at the scale of metres. They interpreted that these ‘reflect the initial isotopic heterogeneity of the source material which has not been obliterated by magmatic processes ...’. Two separate melting events, that differ in age by 4 Ma, have been defined here (Harrison *et al.*,

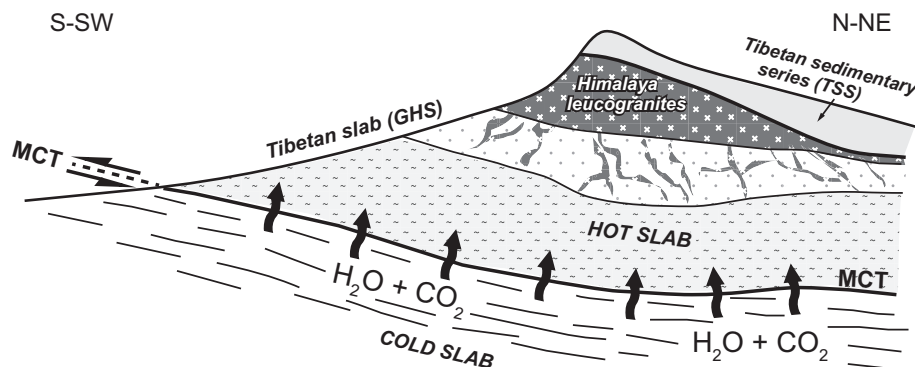


**Fig. 2.** Classic view of anatexis triggered by the overthrust of the GHS and fluids released through metamorphism of the colder LHS (after Le Fort *et al.*, 1987). This could also be the source of metasomatic fluids preceding melting (Guo & Wilson, 2012).

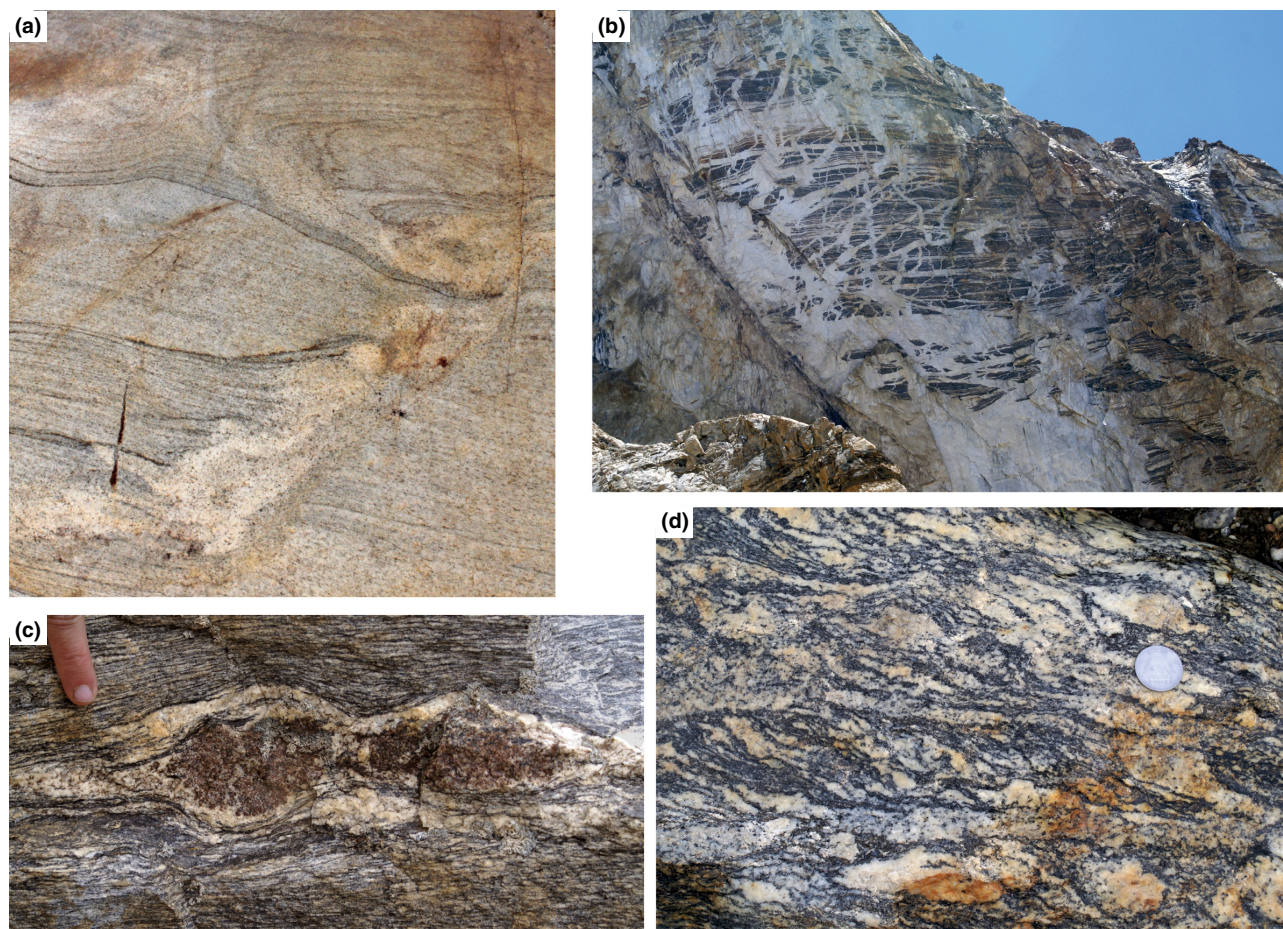


**Fig. 3.** (a) Biotite quartzite, Pandukeshwar Formation, Saraswati valley, Garhwal, showing *in situ* melting while preserving primary sedimentary structures. The protolith is mica-poor and generated small volumes of melt. Leucosomes and source rock lack anhydrous peritectic phases and the low regional peak temperature estimates suggest water-fluxed melting (see Prince *et al.*, 2001). (b) Gumbaranjun intrusive complex: magma accumulation within the Zanskar Shear Zone (or STD) immediately below rocks of the THS. (c, d) Two examples of melting reactions in the Zanskar Range. (c) Large garnet grains in narrow leucosome in orthogneiss suggesting biotite-dehydration melting reaction. The small volume of leucosome and absence of garnet retrogression to biotite suggests loss of melt. Features such as these are only locally preserved. (d) Typical migmatite with ~50% leucosomes and lacking anhydrous peritectic minerals suggesting water-fluxed melting.

1999b): a low-Sr, *c.* 23 Ma phase and a high-Sr, 19 Ma phase. Harrison *et al.* (1999b) argued that the high Rb/Sr ratios of these rocks suggested muscovite-dehydration melting reactions, and raised the question as to how two significant phases of crustal melting may be generated by the same crustal region 4 Ma apart (see also Everest area for two melting events, e.g. Streule *et al.*, 2010). They suggested shear heating as a possible cause. Knesel & Davidson (2002) found that the two melting events have different Sr-isotopic composition and Sr content. They considered disequilibrium melting of the same source rock, and found that the older group was a result of muscovite-dehydration melting, but that the younger group resulted from water-fluxing melting (Fig. 4), suggesting that fluid influx after the end of muscovite-dehydration melting triggered the second melting event.

#### Muscovite- and biotite-dehydration melting

Many sections of the GHS have reached or exceeded metamorphic conditions for muscovite- and biotite-dehydration melting (Table 1). Considerable efforts have been made in determining whether melting occurred on the prograde path, before decompression (e.g. region between Everest and Sikkim), or whether decompression triggered melting (e.g. Langtang). Here, cases that exemplify the range and complexity of melting conditions are reviewed.

#### Langtang

Inger & Harris (1992) argued for two phases of metamorphism in Langtang: (i) an early Barrovian metamorphism resulting in Ky + St assemblages, followed by (ii) heating preceding or during decompression, to

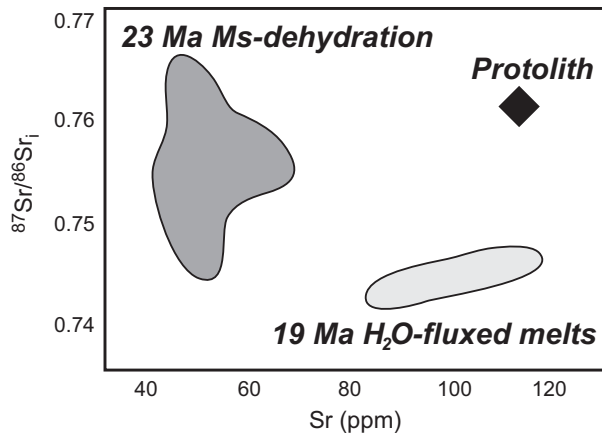


**Fig. 4.**  $^{87}\text{Sr}/^{86}\text{Sr}$  v. Sr content showing bimodal distribution of Manaslu granites, grey fields (after Knesel & Davidson, 2002) corresponding to two different melting events 4 M.yr. apart (Harrison *et al.*, 1999a). Sr content and isotopic composition of the 23 Ma, low-Sr, high- $^{87}\text{Sr}/^{86}\text{Sr}$  granites can be accounted for by muscovite dehydration melting, whereas those of the 19 Ma, high-Sr, low- $^{87}\text{Sr}/^{86}\text{Sr}$  granites can be accounted for by water-fluxed melting. Solid diamond marks the value for modelled source rock for Himalayan granites (from Patiño Douce & Harris, 1998).

sillimanite grade metamorphism and anatexis by muscovite dehydration, producing peritectic Sil + Kfs assemblages in metapelites between 20 and 17 Ma. In this case, melting occurred as the rocks heated from  $710 \pm 30$  to  $760 \pm 30$  °C and decompressed from  $\sim 10$  kbar to  $5.8 \pm 0.4$  kbar, evidenced by cordierite forming quartz symplectite coronas around garnet. Kohn *et al.* (2005) found a range of monazite ages in samples of the region and determined that melting occurred within the MCT as late as 16 Ma (see also Kohn, 2008).

Harris & Massey (1994) argued that for the Langtang region, Sr-isotopes indicated muscovite-dehydration melting of kyanite-bearing schists generated leucogranites that rose >10 km and were emplaced into sillimanite-bearing migmatites close to the STD. Harris *et al.* (1993) used Rb–Sr–Ba contents to argue that the Langtang and Gangotri granites are a result of disequilibrium melting. They have low Rb/Sr values compared to Manaslu and Gopu La granites, and lower than expected values for melts derived from dehydration melting. This could be a result of either: (i) plagioclase fractionation, removing Sr; (ii) the presence of an aqueous fluid in the source, increasing involvement of plagioclase in the melting reaction, or (iii) disequilibrium melting. They argued that fractionation of plagioclase is unlikely, based on the increase of Rb/Sr with Ba, because removal of plagioclase alone would keep Ba constant as Rb/Sr changes. They accepted that the presence of a small fraction of aqueous fluids in the source may have reduced Rb/Sr, and increased melt fractions, but ultimately they argued that the low Rb/Sr values are a result of disequilibrium due to fast melt extraction.

#### Sikkim

The metamorphic record of the GHS in Sikkim indicates that an increase in  $P$ – $T$  was interrupted by nearly isothermal decompression (Neogi *et al.*, 1998; Ganguly *et al.*, 2000; Harris *et al.*, 2004; Rubatto *et al.*, 2013; Sorcar *et al.*, 2014). Unlike elsewhere in the Himalayas, there has been some interleaving between rocks of the LHS and the GHS along the MCT (Mottram *et al.*, 2014a) and other recent papers have placed the MCT in Sikkim within the high-grade rocks due to the existence of a high-strain zone separating rocks with different protolith age and metamorphic histories (Dasgupta *et al.*, 2009; Rubatto *et al.*, 2013). Melting in the lower part of the high-grade sequence (part of the Lesser Himalayas as defined in Dasgupta *et al.*, 2009), started in the presence of an aqueous fluid in the kyanite zone, progressing to muscovite dehydration and then biotite-dehydration melting reactions with increasing temperature (Dasgupta *et al.*, 2009). A similar progression has been inferred for the upper part of the sequence, within the GHS, where metamorphism followed a clockwise metamorphic path reaching a peak of 8–10 kbar and 800 °C, followed by nearly isothermal decompression to  $\sim 5$  kbar, and then isobaric cooling (Harris *et al.*, 1993; Ganguly *et al.*, 2000; Rubatto *et al.*, 2013; Sorcar *et al.*, 2014; Gaidies *et al.*, 2015). According to Rubatto *et al.* (2013), melting started in the prograde path when temperature exceeded  $\sim 700$  °C, continued during isothermal decompression and ended during the isobaric cooling stage. Thus, they argue, decompression was a consequence rather than cause of melting, in contrast to the conclusions of Harris *et al.* (2004).

#### Makalu area: Barun Gneisses decompression melting

In the Makalu region, the GHS is 25–30 km thick, with thick packages of migmatites topped by the Makalu granite complex (Streule *et al.*, 2010). Biotite-dehydration melting took place in the deeper and hotter sections, and muscovite-dehydration melting further up. In parts of the system, melting was a result of heating followed by decompression (Groppo *et al.*, 2012), in other parts, a result of low-pressure, prograde heating, stabilizing cordierite and andalusite in migmatites and granites (Groppo *et al.*, 2010a, 2013; Streule *et al.*, 2010; Visonà *et al.*, 2012).

Groppo *et al.* (2012) investigated two granulite facies samples of Grt + Sil + Ky stromatic migmatites from the deeper parts of the Barun gneiss. They indicate a clockwise  $P$ – $T$  path with an estimated pressure of 10–8 kbar at peak temperature of 800–850 °C, and decreasing pressure structurally upwards. Peak conditions were followed by decompression to  $\sim 7$  kbar. Groppo *et al.* (2012) discussed melting reactions and inferred that melting resulted from muscovite followed by biotite breakdown, and concluded

that 'a significant amount of melt was produced in the Barun Gneiss prior to decompression...'.

#### *Makalu area: low-*P* cordierite leucogranites and migmatites*

In the Makalu region, structurally above the Barun Gneisses of the previous section, Streule *et al.* (2010) investigated cordierite-bearing Makalu granites and migmatites (see also Pognante & Benna, 1993; Goscombe & Hand, 2000; Groppo *et al.*, 2013). They found two phases of crustal anatexis: coarse-grained, *c.* 16 Ma, cordierite leucogranites cut across and overlie 24–21 Ma cordierite-free, Grt + Tur + Ms ± Bt leucogranites. Cordierite leucogranites were likely fed from the migmatitic gneisses, which record decompression evidenced by cordierite coronas around garnet and the gradual upward disappearance of garnet with increased modal content of cordierite (Streule *et al.*, 2010). A pseudosection of a palaeosome indicates that muscovite-dehydration melting occurred at 700 °C at a maximum pressure of only ~6 kbar. Peak conditions were followed by cooling and decompression within the muscovite-dehydration field, that increased melt fraction and stabilized cordierite in granites that crystallized at 700 °C and 4 kbar and crossed the solidus at nearly 600 °C and 2 kbar. These low-*P* granites are closely related in space and time to andalusite-bearing leucogranites (see below).

Groppo *et al.* (2013) investigated migmatites immediately below the leucogranite intrusions over a wider area between Everest and Kangchenjunga, encompassing the Makalu region. The migmatites have poikiloblastic, peritectic and magmatic cordierite, indicating that melting started in the prograde path in the low-*P* stability field of cordierite. They inferred that melting resulted from the breakdown of biotite, reacting with sillimanite and quartz to produce Kfs + Crd + melt at 750–800 °C and 4–6 kbar. They suggested that the cordierite-bearing migmatites could be the source of the andalusite granites that crop out at higher structural levels (Visonà *et al.*, 2012).

#### *Everest to Bhutan: low-*P* andalusite leucogranite*

These leucogranites intrude the upper part of the GHS (and the North Himalayan Domes) and are Ms–Bt leucogranites (±Tur ± Crd ± Sil ±, Ky, and spinel and corundum) (Visonà & Lombardo, 2002; Kellett *et al.*, 2009; Visonà *et al.*, 2012). They have several generations of andalusite (residual, peritectic and magmatic), interpreted to have formed during isobaric heating at pressures below 4 kbar. Inclusions of biotite and sillimanite in peritectic cordierite suggest biotite-dehydration melting reactions (Visonà *et al.*, 2012). Furthermore, sillimanite overgrowing andalusite indicates heating towards biotite-dehydration conditions at low pressure. Andalusite crystallization was favoured by the high F and B content in

these magmas, indicated by fluorite and tourmaline, that suppressed the solidus curve. Metamorphic and magmatic andalusite, and the coincidence in age between andalusite granite, cordierite granite, and migmatitic gneisses, led Visonà *et al.* (2012) and Visonà and Lombardo (2002) to argue that both prograde and retrograde paths occurred at low pressure, as a result of nearly isobaric heating and cooling. Given the 16 Ma age of these leucogranites, Visonà *et al.* (2012) argued that this was the second anatexis event, overprinting the earlier event related to decompression melting.

In summary, cordierite and andalusite granites and migmatites between Everest and Bhutan mark a second melting event a few million years after a first event related to decompression. The second event was characterized by a low-*P* prograde path peaking at biotite-dehydration melting conditions. This low-*P* heating poses interesting questions regarding the heat source for melting at shallow levels.

### **TIMING AND DURATION OF ANATEXIS AND LEUCOGRANITE CRYSTALLIZATION**

Anatexis marks peak metamorphic conditions and the period when rocks are at their weakest, prone to destabilizing the crust. The timing and duration of anatexis therefore provides fundamental constraints for tectonic models of the Orogen. Monazite and zircon in leucogranites and migmatites have been widely dated, and here recent results are reviewed and establish that:

- (a) Most areas record *c.* 10 Ma duration of anatexis and granite generation, typically lasting between 25 and 15 Ma (summary in Leech, 2008).
- (b) Monazite and zircon from individual samples have age spreads covering a significant portion of this 10 Ma period, indicating incomplete resetting and complexities in the recycling and growth of these minerals during anatexis.
- (c) Chemistry of accessory phases has allowed timing the prograde and retrograde paths of the anatexis *P–T* paths, and reveal systematic age changes across strike of the Orogen.

The use of granite ages to bracket the time of movement on the STD is reviewed in the next section.

Monazite is the more commonly dated mineral. During prograde metamorphism allanite reacts to form monazite at ~500 °C, near the garnet isograd (Harrison *et al.*, 1999b) and during melting, monazite is expected to partially dissolve, even at low melting temperature, and regrow during melt crystallization. Zircon, in contrast, is less likely to grow at sub-solidus conditions (Kelsey *et al.*, 2008), so does not record the prograde history. It also dissolves less readily in the melt, preserving inherited ages, and then tends to regrow or form new grains during

magma crystallization, recording magma crystallization ages (Kohn *et al.*, 2015).

The chemistry of monazite (particularly REE, Y and Th) and of zircon (particularly REE), and their response to changes in the modal proportions of garnet, allows linking their ages to prograde and retrograde metamorphic paths, and constrain the duration of anatexis (Horton & Leech, 2013; Lederer *et al.*, 2013; Rubatto *et al.*, 2013; Kohn, 2014; Mottram *et al.*, 2014b). During the prograde path, growth of garnet sequesters Y and Th, leading to their gradual decrease in monazite as it grows. When anatexis starts, monazite dissolves only to crystallize upon magma cooling, when garnet is unstable, forming high-Y and Th rims around older monazite grains. This is used in combination with Eu anomalies in the accessory phases, reflecting the melting of feldspar or its crystallization, to derive the history of anatexis. Recent developments in Ti-in-Zrn geothermometry have been combined with zircon geochronology to determine zircon crystallization temperature (Kellett *et al.*, 2013; Rubatto *et al.*, 2013). As summarized by Kohn (2014, his fig. 9c), the resulting Ti-in-Zrn temperatures are too low, typically lower than the  $P$ - $T$  paths recorded independently.

#### Zanskar, Leo Pargil and West Nepal

Anatexis in Zanskar may have started at *c.* 27 Ma or even earlier (Horton *et al.*, 2015) and continued to *c.* 20 Ma (Noble & Searle, 1995; Dèzes *et al.*, 1999; Walker *et al.*, 1999; Robyr *et al.*, 2006, 2014; Horton & Leech, 2013; Finch *et al.*, 2014; Horton *et al.*, 2015), when it was interrupted by rapid cooling resulting from movement on the STD (Finch *et al.*, 2014), marked by muscovite Ar-cooling ages between 22 and 20 Ma (Walker *et al.*, 1999; Horton *et al.*, 2015). This is further detailed below when constraining movement on the STD.

The Leo Pargil Dome, NW India, is included in this review although it is not strictly part of the GHS, and is more similar to other domes formed by orogen-parallel extension, such as Gurla Mandata and Ama Drime (G.W. Lederer, per. comm.). It is included here because it is a great example of monazite recycling during magmatism (Lederer *et al.*, 2013) relevant to understanding the processes of leucogranite formation. The dome is comprised of high-grade metamorphic rocks with an anatectic core, and formed as a result of orogen-parallel extension and separated from lower grade rocks by the Leo Pargil low-angle, normal shear zone. Leucogranites intrude gneisses and kyanite-garnet schists of the lower section of the shear zone, and decrease in volume upwards towards the low-grade THS rocks in the hangingwall (Langille *et al.*, 2012). Lederer *et al.* (2013) investigated the ages and composition of monazite (U-Th/Pb LA-ICP-MS) and found 'semicontinuous crystallization of monazite from 30 to 18 Ma'.

Each granite sample yielded a range of ages, and the youngest age was interpreted to represent the time of magma crystallization, consistent with cross-cutting relationships in the field. Older ages in each sample comprise a combination of grains inherited from early-formed, partially crystallized melt, and from source metapelites (Fig. 5a). The age range of inherited monazite overlaps with U-Pb (SHRIMP) ages of igneous zircon (Fig. 5b) (Leech, 2008). These contrast with the ages of metamorphic monazite from unmelted rocks that grew during garnet growth between 34 and 30 Ma. Lederer *et al.* (2013) concluded that in the Leo Pargil Dome individual melting pulses lasted 1–2 Ma, and recycled earlier pulses.

Further east, in the Bura Buri granite in West Nepal, Carosi *et al.* (2013) found two monazite age peaks in a leucogranite dyke sample ( $22.8 \pm 0.4$  and  $24.8 \pm 0.5$  Ma) and suggested that they represent two magma pulses. This same sample had monazite cores with ages between 30 and 25 Ma, inherited from the granite source. This granite cuts across the STD and constrains the timing of normal movement (see section on South Tibetan Detachment).

#### Modi Khola (Annapurna) and Langtang, Central Nepal

In Modi Khola, Corrie & Kohn (2011) distinguished four generations of monazite: inherited and/or mixed, early prograde, late prograde, and post-anatectic where the age peaks of each population 'correspond to specific chemistries, and thus to petrological origins' (Fig. 6a). Prograde monazite has low-Y and Th peaks, whereas retrograde has high-Y and overgrows prograde cores. Thus, the age difference between the youngest prograde and the oldest retrograde monazite, brackets the duration of anatexis. They proceeded to show that both the prograde and melt crystallization decreased in age systematically from the uppermost GHS to the lowermost and that this was accompanied by a decrease in peak  $P$ - $T$  conditions. A similar pattern was found also for the Langtang region (Fig. 6b, Kohn *et al.*, 2004).

#### Everest-Makalu-Dinggye Regions

Barrovian metamorphism in the Everest-Makalu region, marked by the growth of new monazite, peaked between 35 and 30 Ma (Simpson *et al.*, 2000; Viskupic & Hodges, 2001; Groppo *et al.*, 2010b; Streule *et al.*, 2010). Leucogranites and migmatites have been dated by numerous authors (e.g. Hodges *et al.*, 1998; Murphy & Harrison, 1999; Simpson *et al.*, 2000; Viskupic *et al.*, 2005; Jessup *et al.*, 2008; Cottle *et al.*, 2009; Streule *et al.*, 2010; Visonà *et al.*, 2012). Magmatism started at *c.* 24 Ma and ended *c.* 16 Ma (see table 1 in Cottle *et al.*, 2015). The late *c.* 16 Ma leucogranites in the Everest region are contemporaneous with sills and dykes in Makalu (Streule *et al.*, 2010) and the 24–16 Ma age range found by

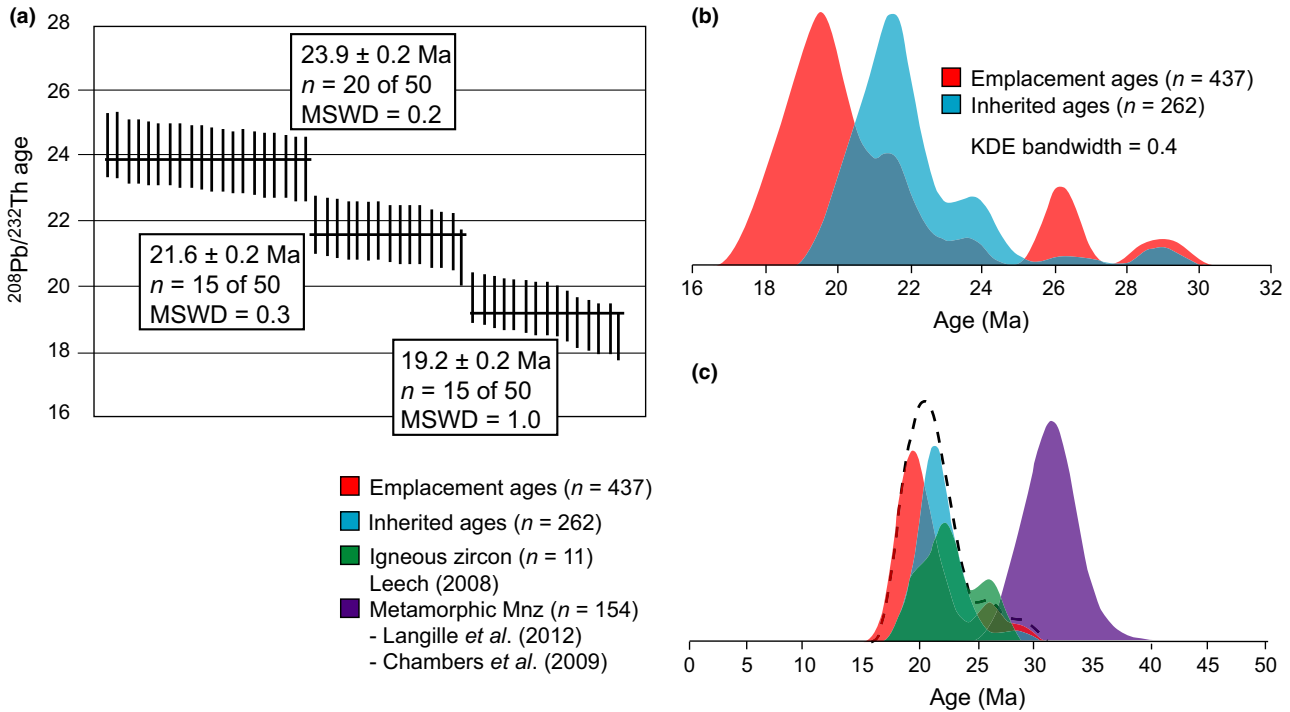
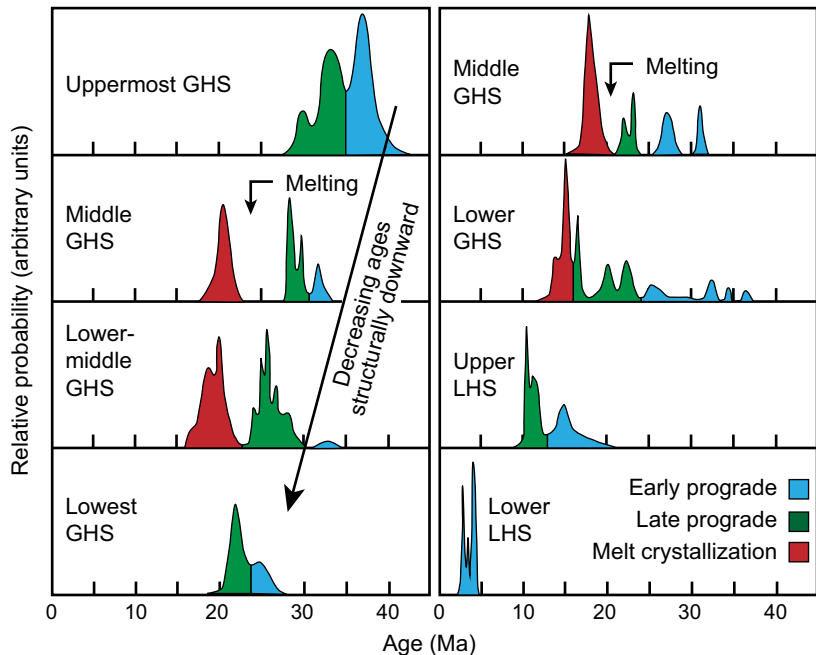


**Fig. 5.** (a) An example of monazite Pb/Th spot ages from a sample from the Leo Pargil Dome defining three distinct age groups indicated by horizontal lines. The youngest group was interpreted to represent granite crystallization ages, the two older groups as inherited from early-formed, partially crystallized magmas. (b) Aggregated results from several samples from Leo Pargil showing the youngest group of monazite ages representing final magma crystallization, partially overlapping with an older age group representing inherited grains. This group coincides with zircon ages and is younger than monazite ages from metamorphic rocks shown in (c). Both zircon and monazite grains were not completely dissolved/re-precipitated during anatexis. Vertical axis is arbitrary and represents relative % of each data set (all figures after Lederer *et al.*, 2013).

Cottle *et al.* (2009) is similar to that found in the Mabja dome (Lee & Whitehouse, 2007) of the North Himalayan leucogranites, suggesting continuity

between the two regions. Migmatite ages reflect those of leucogranites, and Visonà *et al.* (2012) considered the end of the migmatitic stage at *c.* 16 Ma as

**Fig. 6.** Timing of prograde and retrograde (melt crystallization) metamorphism across strike of the Himalayas from uppermost to lowermost GHS and LHS in Modi (left column) and Langtang (right column) sections, based on monazite age and chemistry. Timing of anatexis is between the youngest prograde and melt crystallization ages. Notice systematic younging of the metamorphic cycle towards the base of the GHS (redrawn from Kohn, 2014).



indicative of the end of the south-directed channel flow. The youngest leucogranite intruded at  $12.6 \pm 0.2$  Ma, post-dating ductile deformation on the STD by 4 Ma suggests continued anatexis at depth (Cottle *et al.*, 2009).

The findings of Viskupic *et al.* (2005) for the Everest area are similar to those for the Leo Pargil Dome. Accessory phases dated to between 26 and 23 Ma were found in intrusive leucogranite crystallized at 22–21 Ma. The older ages were interpreted to indicate a prolonged, episodic or continuous melting of the source, mobilized by a later magma extraction. These accessory phases record anatexis predating activity on the MCT and STD. West of the Everest, at Nyalam, melting started as early as 30 Ma and migmatites crystallized first at the structurally highest section of the GHS at *c.* 20 Ma, and last at the base of the GHS at 15 Ma (Leloup *et al.*, 2015).

### Sikkim and East Nepal

Melting in Sikkim and E Nepal has been dated by different methods (Catlos *et al.*, 2004; Harris *et al.*, 2004;

Imayama *et al.*, 2012; Kellett *et al.*, 2013; Rubatto *et al.*, 2013). Dating of monazite and zircon, combined with their chemistry, allowed constraining the timing and evolution of melting (Imayama *et al.*, 2012; Kellett *et al.*, 2013; Rubatto *et al.*, 2013; Mottram *et al.*, 2014b). Unlike other regions, melting here seems to have lasted 15 Ma having started earlier than elsewhere, blurring the boundary between Eo- and Neohimalayan metamorphism (see similar findings in rocks further west in Leloup *et al.*, 2015). Metamorphic GHS rocks yielded U–Pb age ranges of monazite and zircon between 37 and 14.5 Ma and melting is estimated to have lasted from 33 to 16 Ma in E Nepal (Imayama *et al.*, 2012) and from 31 to 17 Ma in north Sikkim, where peak metamorphism and the initiation of melting were diachronous from N to S (Rubatto *et al.*, 2013). The higher structural levels of the GHS reached peak conditions between 26 and 21 Ma compared to between 31 and 27 Ma for the lower levels (Fig. 7a). Rubatto *et al.* (2013) suggested that the time taken by any particular block of rocks to traverse the *P–T* field appropriate for melting was *c.* 5 Ma.

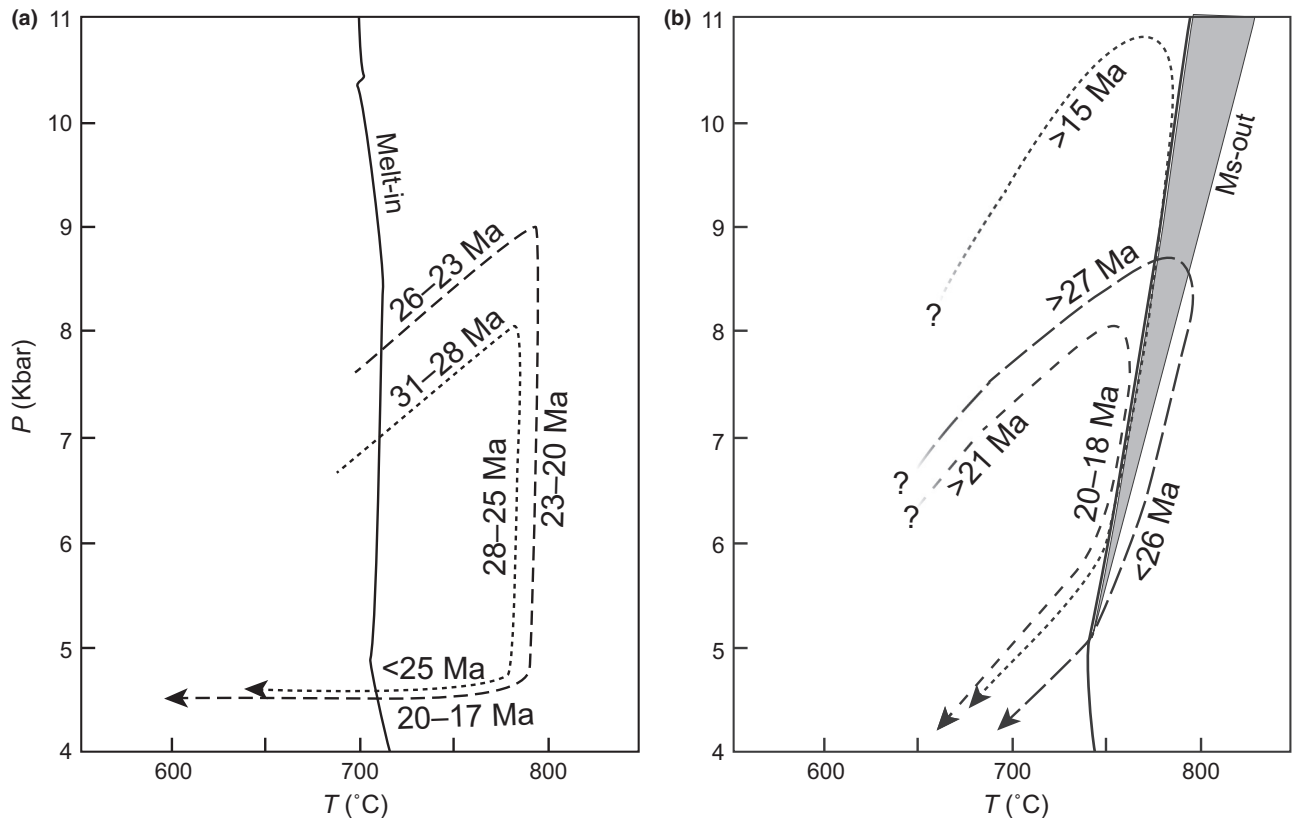


**Fig. 7.** (a) Clockwise *P–T* paths and progression ages for place (a) at the start of the caption Sikkim. Dotted line for a sample from the lower GHS, dashed line for a sample from the upper GHS close to the STD. Simplified from fig. 9 in Rubatto *et al.* (2013). (b) Representative paths and interpreted progression ages from Bhutan. Dotted line (>15 Ma) is from the structurally highest location, short-dashed lines (prograde path >21 Ma followed by decompression at 20–18 Ma) is intermediate and the long-dashed line (prograde path >27 Ma followed by retrograde path <26 Ma) is from the structurally lowest location in the GHS. Simplified from fig. 11 in Zeiger *et al.* (2015). Steep continuous lines are solidus lines from original figures. Ages for prograde and retrograde paths are interpreted from metamorphic and melt crystallization ages obtained from monazite and zircon.

The long age ranges found in individual samples were inferred to indicate continuous or multiple episodes of dissolution/precipitation during a single  $P$ – $T$  cycle as a result of changing metamorphic reactions (Kellett *et al.*, 2013; Rubatto *et al.*, 2013; Mottram *et al.*, 2014b; see also Leo Pargil Dome and the Everest above, and Bhutan below). Like in Zaskar, magmatism in Sikkim ended abruptly, accompanied by rapid cooling between 16 and 14 Ma to *c.* 12 Ma (Kellett *et al.*, 2013). Thus, the GHS in Sikkim went through rapid isothermal decompression during migmatization lasting a few million years at *c.* 25 Ma (Fig. 7a), followed by a period in which it remained hot, until rapid cooling took place some 10 Ma later (Kellett *et al.*, 2013; Rubatto *et al.*, 2013). The northward younging of both the beginning and the end of melting in Sikkim is the opposite to the southward younging found at Modi Khola and Langtang (Kohn *et al.*, 2004; Corrie & Kohn, 2011) and in Bhutan (see below). No current model explains these results.

### Bhutan

Zeiger *et al.* (2015) found an age range in zircon and monazite from 36 to 14–13 Ma for the upper part of the GHS in Bhutan, similar to Sikkim. The older age group, between 36 and 28 Ma, reflects early metamorphism. Zircon in leucosomes suggests protracted melting, with a wide distribution of Miocene zircon ages from individual leucosomes along the concordia. The majority of leucosomes crystallized between *c.* 20 to 18 Ma (see also Carosi *et al.*, 2006). The combination of zircon and monazite U–Pb spot ages with their chemical composition suggest a systematic clockwise temporal evolution with heating to 750–800 °C, and peak pressures between 11 and 8 kbar (Fig. 7b). Contrary to Sikkim and consistent with findings in Nepal (Kohn *et al.*, 2004; Corrie & Kohn, 2011), structurally higher metamorphic rocks went through the clockwise cycle earlier than those at the base, whereas granites become younger to the north (see below; Kellett *et al.*, 2009).

### SOUTH TIBETAN DETACHMENT: TIMING AND DURATION

Exhumation of the GHS and the role of the STD are key in understanding the Orogeny. Timing of motion has been constrained either by rapid cooling of metamorphic rocks in the footwall of the STD (summarized in Kellett *et al.*, 2013, see also discussion in Leloup *et al.*, 2015), or bracketed by the age of deformed and undeformed granites within the STD. Here, examples published since the review by Godin *et al.* (2006) are reviewed, and focus specifically on those that constrain the duration of movement on the STD based on granite ages (Table 2). The time of ductile movement on the STD varies and was generally short-lived. In some places, anatexis immediately

**Table 2.** Summary of recent works constraining duration of normal ductile shearing on the STD based on granite U–Th–Pb ages. There is no systematic variation from W to E. For a comprehensive list of pre-2006 studies, see Godin *et al.* (2006).

Location (from W to E)	Constraints	Observations	Reference
Zaskar	Upper bound <i>c.</i> 26 Ma, granite monazite age recording thrusting. Lower bound 20–21 Ma, undeformed granite cross-cutting STD, combined with Ar/Ar-cooling ages		Finch <i>et al.</i> (2014), Horton <i>et al.</i> (2015) see also Dézes <i>et al.</i> (1999) and Walker <i>et al.</i> (1999)
West Nepal, Bura Buri	23–25 Ma monazite age from undeformed granite cross-cutting STD	Two-mica tourmaline leucogranite	Carosi <i>et al.</i> (2013)
Rongbuk (N Everest)	>17 to 16 Ma constrained by monazite age from deformed and undeformed leucogranites		Cottle <i>et al.</i> (2015) see also Murphy & Harrison (1999)
Dinggye (northeast of Makalu)	16 Ma deformed granite (monazite + zircon ages), deformation ends between 13.6 and 11 Ma	Timing based on structural and petrographic consideration	Leloup <i>et al.</i> (2010)
Bhutan	<15 Ma for inner STD (monazite age) <11 Ma for outer STD (monazite age)	750–800 °C 11–8 kbar Clockwise $P$ – $T$	Edwards & Harrison (1997), Kellett <i>et al.</i> (2009), Zeiger <i>et al.</i> (2015)

preceded normal movement, in others it may have been a response to it. These variations suggest that initiation of normal movement on the STD was a regional response to the dynamic and kinematic history of the Orogen where anatexis played a secondary role, modulating the local response (see Discussion).

Granites locally cross the STD and intrude the THS (e.g. western Nepal and Garhwal Himalaya, Sachan *et al.*, 2010; Carosi *et al.*, 2013; and see also debate in and around Rongbuk valley, north of the Everest, Hodges *et al.*, 1998; Murphy & Harrison, 1999). However, the accumulation of granite underneath or within the STD (Scaillet *et al.*, 1995a; Weinberg & Searle, 1999; Searle *et al.*, 2006; Carosi *et al.*, 2013; Lederer *et al.*, 2013; Finch *et al.*, 2014) suggests it was an impediment for magma migration, possibly a combined result of a stronger foliation anisotropy and the thermal and rheological barrier represented by the cold rocks of the THS.

In Zaskar, the duration of movement on the STD has been constrained by the switch from thrusting to normal movement during anatexis and by undeformed leucogranites cross-cutting the STD (Finch *et al.*, 2014). The STD (or Zaskar Shear Zone) is a 1–2 km thick band of mylonitic gneisses and Miocene leucogranites, with a top-to-northeast normal movement sense (Herren, 1987; Pognante & Lombardo, 1989). It overprints thrusting recorded on both its footwall and hangingwall (Finch *et al.*, 2014). Robyr *et al.* (2006) dated monazite in migmatites and leucogranites of the footwall and found ages ranging

from 26.6 to 19.8 Ma. They suggested that melting was a response to decompression related to normal movement and inferred that extension started shortly before 26.6 Ma. In contrast, Finch *et al.* (2014) found that anatexis started during thrusting and continued as deformation switched to normal movement, and that therefore anatexis was not a response to exhumation and decompression. They dated monazite from three leucogranite samples. The oldest sample recorded only early thrusting, the intermediate sample was a mylonitic leucogranite from the STD, and the youngest sample was an undeformed leucogranite cross-cutting the STD (Finch *et al.*, 2014). The monazite ages of all three samples define a similar age range as that found by Robyr *et al.* (2006), between 26 and 20 Ma, with the age peak varying from sample to sample. The broad and coincident age range indicates that monazite records *c.* 6 Ma duration of peak metamorphism interpreted to mark anatexis (Robyr *et al.*, 2006; Finch *et al.*, 2014). Finch *et al.* (2014) concluded that the switch from thrusting to normal movement must have occurred during this period and that normal movement must have ended by *c.* 21–20 Ma, dated by the crystallization age of the undeformed leucogranite, which coincides within error with  $^{40}\text{Ar}/^{39}\text{Ar}$  muscovite cooling ages (Dèzes *et al.*, 1999; Walker *et al.*, 1999; Horton *et al.*, 2015). Together, these results constrain the maximum duration of normal movement to  $<6$  Ma between *c.* 26 and 20 Ma (Finch *et al.*, 2014; Table 2).

Further east, at Malari in Garhwal Himalaya, the end of ductile deformation was constrained by the age of undeformed granites cutting the STD (Sachan *et al.*, 2010). However, more recently, Jain *et al.* (2014) found that the Malari granite records ductile thrusting overprinted by normal movement, as well as brittle deformation, casting doubt on this age constraint. In West Nepal, the Bura Buri leucogranite was dated to an age range of 25–23 Ma (Carosi *et al.*, 2013). These ages limit the time available for contemporaneous motion of the STD and MCT to only 1–2 Ma. Cottle *et al.* (2015) were able to bracket more tightly the end of movement on the ductile section of the STD in the Rongbuk valley (Everest region). Here, *c.* 16.4 Ma granites have been folded, whereas 15.6 and 15.4 Ma granites are undeformed (see also Murphy & Harrison, 1999; Table 2).

In Bhutan, 15.5 Ma sheared leucogranites constrain the lower bound for ductile movement on the outer section of the STD, exposed further south than the inner section, where sheared leucogranites suggest that it was active until at least *c.* 11 Ma, and later overprinted by brittle faulting (U–Pb SHRIMP zircon ages, Kellett *et al.*, 2009). This is in agreement with the  $12.5 \pm 0.4$  Ma Th–Pb monazite ages of a sample from the lowermost part of the Khula Kangri granite, sheared by the STD at the Bhutan–Tibet border (Edwards & Harrison, 1997). The younging of granites to the north from 15.5 to 12–11 Ma in

Bhutan (Kellett *et al.*, 2009) reflects a similar trend found by Cottle *et al.* (2009) east of the Everest, and suggests a possible regional younging towards the North Himalayan granites (Zhang *et al.*, 2004).

The use of granite deformation to constrain timing of movement of shear zones is not always straight forward. It assumes that deformation is recorded by granites but this depends on: (i) the ratio between magma cooling and strain rates, where fast cooling of a syn-kinematic granite may inhibit straining; (ii) the strength contrast between solid granite and surroundings, where competent granites deflect deformation; (iii) the erasing of high-*T* deformation by pervasive low-*T* deformation; (iv) the size, and shape of magmatic bodies, where narrow dykes are more easily deformed than large bodies; (v) localization of deformation to a section of a large leucogranite body, typically the margins (see Bura Buri leucogranite, Carosi *et al.*, 2013); and (vi) grain size and modal fraction of mica. For example, pegmatitic dykes may lack visible deformation even if they are pre- or syn-kinematic (e.g. Leloup *et al.*, 2013).

The full picture of the timing and duration of ductile motion on the STD (Table 2; Godin *et al.*, 2006) has yet to emerge. The current data have several weaknesses such as: (i) incomplete and variable constraints along the length of the STD, (ii) only lower or upper bound ages are available for many locations, (iii) migration of movement locus, (iv) uncertainties regarding the final crystallization age of leucogranites, and (v) questions regarding the structural record of granites (as discussed in paragraph above). Despite these issues, it seems that movement on the STD is broadly contemporaneous with Miocene anatexis, but varies from place to place with no particular systematics (see also Godin *et al.*, 2006). This suggests that initiation and duration of normal movement depends on the strain history along and across strike of the Orogen (Kellett *et al.*, 2009). This is an important conclusion: diachronous and non-sequential normal movement on the STD would tend to destroy the well-defined arc shape of the Orogen and its internal structures. In order to maintain this coherence, localized movement on parts of the STD must be compensated elsewhere in the Orogen.

#### KARAKORAM MIOCENE LEUCOGRANITES AND MIGMATITES: A COMPARISON

This section summarizes the literature on the Miocene anatexis and related leucogranite cropping out along the Karakoram shear zone (Fig. 1). The aim is to illustrate similarities and differences to the GHS (see Searle *et al.* (2010) for a review of Karakoram leucogranites). Like the GHS, the Karakoram shear zone and surroundings record 10 Ma of syn-tectonic magmatism in the form of migmatites and batholith growth, broadly contemporaneous to anatexis in the GHS (e.g. Searle *et al.*, 1998; Weinberg, 1999; Phillips, 2008; Boutonnet

*et al.*, 2012). Unlike the GHS, Karakoram leucogranites are sourced from a juvenile 100–60 Ma calcalkaline batholith as well as metasedimentary rocks, which imparts different isotopic compositions and zircon inheritance. It also differs fundamentally in how magma migrates and accumulates.

### Anatectic conditions

The Karakoram shear zone is a lithospheric-scale, dextral shear zone, north of the Indus-Tsangpo suture zone, from Tibet through Ladakh in NW India and into Pakistan (Searle *et al.*, 1998; Phillips *et al.*, 2004; Leloup *et al.*, 2011; Boutonnet *et al.*, 2012). There is evidence that Miocene movement on the shear zone actively promoted melting, creating a permeable channel for fluid ingress that triggered water-fluxed melting, and a channel for magma extraction through dyke networks that fed the Karakoram Batholith (Weinberg & Mark, 2008; Weinberg *et al.*, 2009; Reichardt *et al.*, 2010; Weinberg & Regenauer-Lieb, 2010; Reichardt & Weinberg, 2012a). The shear zone most likely acted as a fluid and heat channel in the Miocene as it still does today, linking the mantle to the surface (Klemperer *et al.*, 2013).

Melting in Pakistan has been interpreted to result from biotite dehydration (summarized in Searle *et al.*, 2010). In NW India peak metamorphism reached upper amphibolite conditions (~700–750 °C and ~4–5 kbar; Rolland & Pêcher, 2001) and melting has been interpreted to result from an influx of aqueous fluids, given that the biotite-rich clastic sequence melted without producing obvious peritectic minerals, and melting of the calcalkaline granitoids diorite produced peritectic hornblende (Weinberg & Mark, 2008). Some hornblende has been transferred from the source to the Karakoram batholith, forming a

hornblende-leucogranite body within the more typical two-mica + Grt + Tur leucogranite. The filtering out of peritectic hornblende gave rise to leucogranites with high values of La/Yb, similar to adakites (Reichardt & Weinberg, 2012b).

There are two other interesting aspects of this anatectic region. The first is that it provides a rare opportunity to follow magma from source, through a complex dyke network, to the batholith, ~50 km away along strike of the shear zone (Weinberg & Regenauer-Lieb, 2010; Reichardt & Weinberg, 2012a). In contrast with the much smaller stocks and sills developed in the GHS, here the steep strike-slip shear zone facilitated the feeding of a batholith, as will be discussed below. The second is that leucogranites have hybrid Nd and Sr-isotopic signatures, unlike the very radiogenic Himalayan leucogranites. Reichardt *et al.* (2010) found this was a result of mixing between anatectic magmas from a young and relatively juvenile calcalkaline batholith and magmas from a sedimentary sequence with typical crustal values. This juvenile component is also reflected in the positive  $\epsilon_{\text{Hf}}$  values of zircon (Horton & Leech, 2013).

### Timing and duration of anatexis

Leucogranites and migmatites of the Karakoram Range have been extensively dated in NW India (e.g. Searle *et al.*, 1998; Phillips *et al.*, 2004; Ravikant, 2006; Jain & Singh, 2008; Ravikant *et al.*, 2009; Upadhyay, 2009; Reichardt *et al.*, 2010; Leloup *et al.*, 2011; Boutonnet *et al.*, 2012; Horton & Leech, 2013; Sen *et al.*, 2014) and its continuation in Tibet (Lacassin *et al.*, 2004; Valli *et al.*, 2007, 2008; Wang *et al.*, 2012) and Pakistan (Parrish & Tirrul, 1989; Schärer *et al.*, 1990; Mahéo *et al.*, 2009). Granitic magmatism lasted between 26 and 13 Ma, with three separate peaks (Boutonnet *et al.*, 2012). The youngest

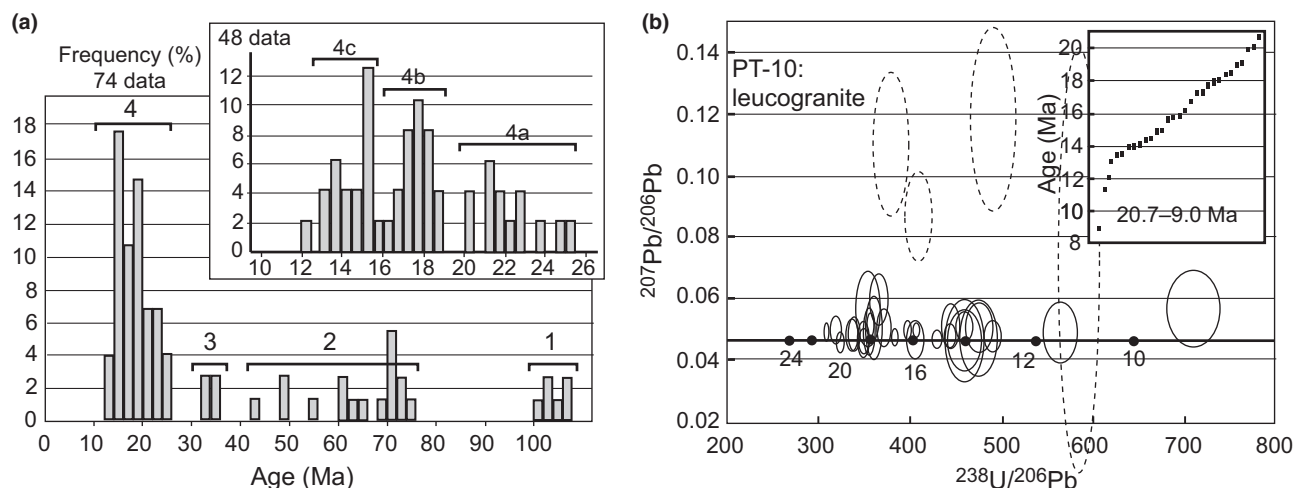


**Fig. 8.** (a) Compilation of published U–Pb ages along the Karakoram shear zone (from Boutonnet *et al.*, 2012). Numbers 1–4 represent four age groups. Group 4 represents magmatic ages and define three subgroups (inset). (b) U–Pb (LA-ICP-MS) zircon age distribution of Karakoram leucogranite sample PT10 (from Horton & Leech, 2013).

peak corresponds mostly to leucocratic and pegmatitic dykes. These granites also include older inherited zircon ages (Fig. 8), with a concentration of ages between 100 and 60 Ma, corresponding to the ages of the calcalkaline Muglib Batholith, that was involved in Miocene leucogranite generation (Reichardt *et al.*, 2010; Reichardt & Weinberg, 2012a; Horton & Leech, 2013), as well as the neighbouring Ladakh Batholith (Weinberg & Dunlap, 2000).

The duration of magmatism is also reflected in the age ranges obtained from single samples. For example, sample PT-10 in Fig. 8b yielded an age range between 21 and <13 Ma. Based on zircon chemistry (in particular Yb/Gd *v.* Hf trends), Horton & Leech (2013) interpreted the range to reflect a protracted period of fractionation during cooling, or alternatively mixed zircon populations.

Similar to the literature about the time of initiation of the STD, the age and deformation state of Karakoram leucogranites are central to discussions regarding the timing of initiation of the Karakoram shear zone (e.g. Leloup *et al.*, 2013). Some leucogranites are unfoliated, suggesting they were post-kinematic, while others only record low-temperature deformation suggesting they are pre-kinematic and were already cold when deformed (Phillips *et al.*, 2004). However, interpretations based on the structural record of granites can be ambiguous (see section on South Tibetan Detachment), as exemplified by a pegmatite dike cropping out within the Karakoram shear zone. This is unfoliated and has been interpreted as post-kinematic; however, the pegmatite grades along strike into a foliated finer grained granite making the dyke either pre- or syn-kinematic (as argued by Leloup *et al.*, 2013).

## DISCUSSION

One of the most exciting recent developments is the increased ability to link zircon and monazite ages with their chemistry (REE, Y and Th) in order to determine timing of prograde metamorphism, anatexis and subsequent cooling. This has helped define: (i) the protracted duration of anatectic events, (ii) the recycling of accessory phases formed earlier in the metamorphic and anatectic cycle, (iii) the thermal evolution of sections of the Himalayas and (iv) constrain the timing of motion on the STD.

### Protracted anatexis and recycling during magmatism

In most anatectic regions investigated, magmatism lasted *c.* 10 Ma between 25 and 15 Ma. Each new paper reinforces this pattern while emphasizing how a particular area deviates from this central theme. Many regions record a semi-continuous record of magmatism (Karakoram, Sikkim, Leo Pargil), others cover a shorter range, interrupted by exhumation and cooling (Zanskar at 20 Ma), and yet others record

two distinct anatectic and magmatic events (Makalu: at 24–21 Ma and at 16 Ma; Manaslu: at 23 Ma and at 19 Ma).

Most interestingly, a single leucogranite or migmatite sample will typically have a broad range of ages, covering a large part of the total duration of magmatism (Horton & Leech, 2013; Kellett *et al.*, 2013; Rubatto *et al.*, 2013; Finch *et al.*, 2014; Horton *et al.*, 2015). While the range of monazite ages may reflect the duration of peak conditions beyond 500 °C, that of zircon tend to reflect the duration of anatexis. Thermodynamic studies raise the expectation that early-formed monazite would be consumed early and record only magma crystallization, while zircon would be preserved during melting and grow further during crystallization (Kelsey *et al.*, 2008; Spear & Pyle, 2010; Yakymchuk & Brown, 2014). This difference has been used efficiently to map out the evolution of some areas (Lederer *et al.*, 2013), but the pattern of ages is seldom as simple as expected (Rubatto *et al.*, 2013; Kohn, 2014). There are many questions regarding the preservation of age ranges in leucogranite and migmatite samples, all of which refer back to complexities in the stability history of zircon and monazite during granite genesis. A number of variables control their stability, from  $P$ – $T$ – $X_{\text{H}_2\text{O}}$  fluctuations, efficiency of melt segregation, and evolving melt and solid chemistry during magma history. While there have been significant developments in understanding the behaviour of zircon and monazite during anatexis, new insights into the genesis of leucogranites will be gained through better understanding their behaviour in a dynamic environment, involving magma extraction and evolving chemistry.

Different hypotheses have been suggested to explain these age ranges for the Himalayan and Karakoram leucogranites: (i) multiple events of partial resorption and regrowth of monazite and zircon during anatexis due to evolving metamorphic reactions (Rubatto *et al.*, 2013), (ii) physical remobilization of early-formed grains in migmatites and leucogranites by new magma pulses, in an environment of fluctuating melt fraction (Viskopic *et al.*, 2005; Lederer *et al.*, 2013), (iii) mixing of ages due to hybridization and magma mixing (Hasalová *et al.*, 2013), and (iv) prolonged fractionation and cooling of granites (Horton & Leech, 2013). Combined, the data suggest that the volumes of melt present in the crust at any time were relatively small, being accumulated, reworked and remobilized several times over the duration of anatexis.

### Magma migration and emplacement: Comparison between Himalayas and Karakoram

The injection complexes formed by the Himalayan and Karakoram leucogranites are a result of pervasive magma migration (Weinberg & Searle, 1998; Hasalová *et al.*, 2013) but they are significantly

different from each other. The sub-vertical attitude of the Karakoram shear zone contrasts with the low-angle foliation of the GHS, exerting different controls on magma migration. In the Karakoram, steep foliation favours the development of a dyke swarm that drains the source and feeds plutons and the Karakoram-Baltoro Batholith (Weinberg *et al.*, 2009; Reichardt & Weinberg, 2012a), up to 10 km wide and 300 km long (Searle *et al.*, 2010). In contrast, migration of Himalayan leucogranite magmas is hampered by the low-angle foliation, so they tend to form stocks or kilometre-thick sills of limited lateral extent, atop injection complexes in the higher reaches of the GHS (e.g. Gangotri, Manaslu, Makalu plutons, or the ballooned sill at Nuptse) where their vertical migration was further inhibited by the thermal barrier imposed by the STD, as discussed earlier.

### Heat sources

The heat source for anatexis has been widely debated (Molnar *et al.*, 1983; England *et al.*, 1992; Harrison *et al.*, 1998) and the discussion will not be replicated here. In the absence of significant advection of heat through mantle mafic magma intrusions, a number of alternative sources have been considered to explain the high temperatures reached in the GHS, including high heat flux from below, shear heating, the role of heat producing elements, and the lower conductivity of the low-grade THS (Jaupart & Provost, 1985). The most likely explanation is a combination of many of these factors (Molnar *et al.*, 1983). The presence of migmatites recording low-*P* anatexis needs some consideration. There are two distinct cases. The first is the one in which rocks underwent isothermal decompression, advecting heat (many areas from Zanskar to Sikkim). The other, more troubling case is when both the prograde and retrograde path of migmatites took place at low pressure (<4 kbar), such as for the Everest and Kangchenjunga regions (e.g. Visonà *et al.*, 2012; Groppo *et al.*, 2013). This requires a steep geothermal gradient typically found only in extensional settings, or in magmatic arcs above subduction zones. This may be a response to heat advection through rapid exhumation of rocks beneath those regions of shallow melting (Visonà *et al.*, 2012).

### STD activation

The section entitled 'South Tibetan Detachment: timing and duration' and Table 2 summarize recent studies that, added to older ones, show that the activation and duration of motion on the STD varies along strike. For example, in some places significant exhumation was already occurring at *c.* 27 Ma (Sikkim, Rubatto *et al.*, 2013; and a little later in Zanskar, Finch *et al.*, 2014; see also Leloup *et al.*, 2015); in other places the STD was no longer active after 23 Ma (western Nepal, Carosi *et al.*, 2013) or 20 Ma

in Zanskar, whereas in others it was active until *c.* 16 Ma (Everest) or *c.* 13 Ma (Bhutan, Kellett *et al.*, 2013). This contrasts with the long activity on the MCT (Daniel *et al.*, 2003; Catlos *et al.*, 2004). Models proposing that the simultaneous movement on the MCT and STD during the Miocene (*c.* 24–16 Ma) played a major role in the exhumation of the GHS (Godin *et al.*, 2006) need to be fine-tuned to take this variability into account. The recent findings of significant internal discontinuities within the GHS in Sikkim (Rubatto *et al.*, 2013) and West Nepal (Montomoli *et al.*, 2013, 2015) also need to be taken into account, particularly with regards to understanding the temporal evolution of metamorphism across the arc: down section younging such as for Modi Khola, Langtang and Bhutan, or up section younging such as for Sikkim and western Bhutan.

### Different timing for anatexis and STD activation: a self-organized response to driving forces

The relative timing between anatexis and decompression has been the basis for different models for GHS exhumation. Some authors argue that decompression triggered melting (Pognante & Benna, 1993; Vance & Harris, 1999), and emphasized the genetic link between ductile activation of the STD, decompression and widespread crustal anatexis (see Cottle *et al.*, 2009). Other authors have suggested that the prograde path led to melting, which triggered relaxation and decompression (Streule *et al.*, 2010; Groppo *et al.*, 2012; Rubatto *et al.*, 2013; Finch *et al.*, 2014). In both cases, decompression leads to increased melt fraction, weakening of the rock mass and possibly accelerating decompression.

Did exhumation trigger melting or melting trigger exhumation? Neither. An alternative view is to consider that exhumation of the GHS was a result of the regional maturation of the Orogen, responding to its entire evolutionary history and not solely to the start of anatexis. At *c.* 30–25 Ma, the crust had thickened sufficiently and its thermal and rheological structure were such that the system became unstable and evolved towards exhumation. At that time significant sections of the crust were close to their local solidus conditions and the relative timing between the initiation of exhumation and melting were modulated by local conditions. While at the local scale there may be a cause and effect relationship between the two, at the regional scale they were both a response to the broader evolution and underlying destabilization of the belt. Local variations impacted on the relative timing of anatexis, the nature of the melting reactions, the extent and speed of exhumation, as well as local geometry and strain distribution. However, these were second-order responses super-imposed on the first-order evolution of the Orogen.

A similar view can be applied to understanding variations on the timing and duration of motion on

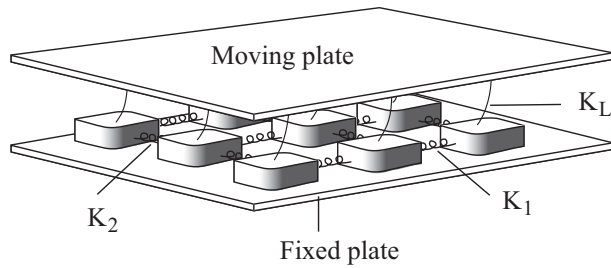


**Fig. 9.** Burridge-Knopoff spring-block model (modified after Olami *et al.*, 1992): interconnected sliders on a frictional base. Each slider is linked to its four nearest neighbours by springs and upwards to a rigid driving plate. Relative movement between the two plates drive motion of the sliders. This dynamic system leads to a quasi-static motion of the system although the motion of individual sliders is unpredictable.  $K_1$ ,  $K_2$ , and  $K_L$  are elastic constants.

the STD (Table 2). These variations suggest that the STD was not a coherent plane but that it developed and accommodated movement as required by local conditions. Yet, the STD as well as the Himalayas and its major internal structures, form well-defined Orogen-wide arcs, with a 100-km scale sinuosity expressed as salients and recesses. Although active at different times, these 100-km scale structures contribute to the structuring of the STD and the orogeny as a whole.

The self-organizing seismic motion of faults might be an appropriate analogue for the mechanisms controlling the evolution of these mountains. Seismic fault motion is modelled by the Burridge-Knopoff spring-block model (e.g. Olami *et al.*, 1992) where a set of sliders resting on a plane, are interconnected by springs, and are linked upwards by another set of springs to a sliding plate (Fig. 9). The movement of single sliders in this set-up occurs at different times and by different magnitudes. While detailed motion of each slider is unpredictable, the system as a whole develops a self-organized aggregate behaviour, in order to balance the accumulation and dissipation of energy between the sliding plates, and allows the system to reach a dynamic equilibrium at nearly steady-state velocity.

The forward motion of the Himalayan orogeny is an expression of the conservation of energy, balancing accumulation of potential energy and dissipation, as identified by Hodges (2000). Like the slider-model, the geological evolution of sections within the deforming orogen is variable and unpredictable. Yet, the large scale response is a steady-state forward movement of the entire belt. In this sense, the Orogeny as a whole responds as a single self-organized structure.

## CONCLUSIONS

Migmatites and leucogranites are broadly contemporaneous across the length of the GHS and the Karakoram, starting some 30 Ma after initial collision and lasting 5–15 Ma. This duration is commonly

recorded also by accessory minerals in a single sample, and interpreted to represent multiple melting events, mixing and remobilization of early-formed magmas with recycling of early crystallized accessory phases, and complex assimilation and growth of the accessory phases during melting.

Melting reactions and  $P$ - $T$ - $X_{H_2O}$  conditions varied across the belt, with examples of water-fluxed melting (Zaskar and Karakoram), muscovite-dehydration melting (Central Nepal) and biotite-dehydration melting (Sikkim, Everest and Makalu). Over two decades ago, one of the main problems in Himalayan metamorphic petrology was explaining the source of heat for anatexis (Inger & Harris, 1992). This problem remains just as relevant today, particularly for explaining the low- $P$  prograde path and melting recorded by cordierite- and andalusite-bearing anatectic rocks.

The low-angle crustal anisotropies in the Himalayas and the barrier imposed by the cold rocks above the STD, inhibited magma extraction and accumulation, favouring diffuse melt migration and local accumulation. In contrast, the transcurrent Karakoram shear zone provided efficient magma pathways and gave rise to the large Karakoram-Baltoro Batholith. The Karakoram shear zone still active today, is a transfer channel of fluids from the mantle to the surface, and may have done so ever since its initiation in early Miocene (>25 Ma), triggering water-fluxed melting at that time.

This paper concurs with Hodges (2000) that 'the Himalaya and Tibet may be the best available laboratory for exploring how feedback relationships among structural, thermal, and erosional processes dictate the behaviour of a collisional system'. The message of the geological record is that, despite the first-order simplicity of the Himalayas, with structures and strata forming a continuous arc, there are significant and apparently disordered variations along strike. Within a general clockwise  $P$ - $T$  path in the GHS, migmatites record differences in amount of exhumation, as well as conditions, timing and duration of anatexis. Likewise, the STD was active at different times and for different periods. These differences suggest that both anatexis and normal shearing, were local, second-order variations imposed on a first-order response to the dynamics driving the Orogen. In conclusion, like a system of interconnected springs and sliders under stress, exhumation and forward movement of the Himalayan front is a self-organized expression of the dissipation of the accumulated potential energy of the thickened crust, controlled by the kinematic boundary conditions imposed by the continuous northward indentation of India into Asia.

## ACKNOWLEDGEMENTS

I thank M. Finch and N. Hunter for reviewing an early version of the manuscript. I also thank F. Capitanio

for helping me express the self-organized properties of the Himalayas. R. Carosi, C. Groppo and D. Kellett are thanked for careful and helpful reviews and S. Bhowmik and D. Robinson for their editorial support.

## REFERENCES

- Beaumont, C., Jamieson, R.A., Nguyen, M.H. & Lee, B., 2001. Himalayan tectonics explained by extrusion of a low-viscosity crustal channel coupled to focused surface denudation. *Nature*, **414**, 738–742.
- Bendick, R. & Bilham, R., 2001. How perfect is the Himalayan arc? *Geology*, **29**, 791–794.
- Boutonnet, E., Leloup, P.H., Arnaud, N., Paquette, J.L., Davis, W.J. & Hattori, K., 2012. Synkinematic magmatism, heterogeneous deformation, and progressive strain localization in a strike-slip shear zone: the case of the right-lateral Karakorum fault. *Tectonics*, **31**, TC4012.
- Burg, J.P. & Chen, G.M., 1984. Tectonics and structural zonation of southern Tibet, China. *Nature*, **311**, 219–223.
- Burg, J.P., Brunel, M., Gapais, D., Chen, G.M. & Liu, G.H., 1984. Deformation of leucogranites of the crystalline Main Central Sheet in southern Tibet (China). *Journal of Structural Geology*, **6**, 535–542.
- Carosi, R., Montomoli, C., Rubatto, D. & Visonà, D., 2006. Normal-sense shear zones in the core of the Higher Himalayan crystallines (Bhutan Himalaya): evidence for extrusion? In: *Geological Constraints on Channel Flow and Ductile Extrusion as an Important Orogenic Process – Himalaya-Tibetan Plateau* (eds Law, R.D., Searle, M.P. & Godin, L.), *Geological Society, London, Special Publications*, **268**, 425–444.
- Carosi, R., Montomoli, C. & Visonà, D., 2007. A structural transect in the Lower Dolpo: insights on the tectonic evolution of Western Nepal. *Journal of Asian Earth Sciences*, **29**, 407–423.
- Carosi, R., Montomoli, C., Rubatto, D. & Visonà, D., 2013. Leucogranite intruding the South Tibetan Detachment in western Nepal: implications for exhumation models in the Himalayas. *Terra Nova*, **25**, 478–489.
- Carosi, R., Montomoli, C., Langone, A. *et al.*, 2015. Eocene partial melting recorded in peritectic garnets from kyanite-gneiss, Greater Himalayan sequence, central Nepal. *Geological Society, London, Special Publications*, **412**, 111–129.
- Catlos, E.J., Dubey, C.S., Harrison, T.M. & Edwards, M.A., 2004. Late Miocene movement within the Himalayan Main Central Thrust shear zone, Sikkim, north-east India. *Journal of Metamorphic Geology*, **22**, 207–226.
- Coleman, M.E., 1998. U-Pb constraints on Oligocene-Miocene deformation and anatexis within the Central Himalaya, Marsyandi Valley, Nepal. *American Journal of Science*, **298**, 553–571.
- Corrie, S.L. & Kohn, M.J., 2011. Metamorphic history of the central Himalaya, Annapurna region, Nepal, and implications for tectonic models. *Geological Society of America Bulletin*, **123**, 1863–1879.
- Cottle, J.M., Searle, M.P., Horstwood, M.S.A. & Waters, D.J., 2009. Timing of midcrustal metamorphism, melting, and deformation in the Mount Everest region of southern Tibet revealed by U-(Th)-Pb geochronology. *Journal of Geology*, **117**, 643–664.
- Cottle, J.M., Searle, M.P., Jessup, M.J., Crowley, J.L. & Law, R.D., 2015. Rongbuk re-visited: geochronology of leucogranites in the footwall of the South Tibetan Detachment System, Everest Region, Southern Tibet. *Lithos*, **227**, 94–106.
- Daniel, C.G., Hollister, L.S., Parrish, R.R. & Grujic, D., 2003. Exhumation of the Main Central Thrust from lower crustal depths, eastern Bhutan Himalaya. *Journal of Metamorphic Geology*, **21**, 317–334.
- Dasgupta, S., Chakraborty, S. & Neogi, S., 2009. Petrology of an inverted Barrovian sequence of metapelites in Sikkim Himalaya, India: constraints on the tectonics of inversion. *American Journal of Science*, **309**, 43–84.
- Deniel, C., Vidal, P., Fernandez, A., LeFort, P. & Peucat, J.-J., 1987. Isotopic study of the Manaslu granite (Himalaya, Nepal): inferences on the age and source of Himalayan leucogranites. *Contributions to Mineralogy and Petrology*, **96**, 78–92.
- Dèzes, P.J., Vannay, J.-C., Steck, A., Bussy, F. & Cosca, M., 1999. Synorogenic extension: quantitative constraints on the age and displacement of the Zaskar shear zone (northwest Himalaya). *Geological Society of America Bulletin*, **111**, 364–374.
- Edwards, M.A. & Harrison, T.M., 1997. When did the roof collapse? Late Miocene north-south extension in the high Himalaya revealed by Th-Pb monazite dating of the Khula Kangri granite. *Geology*, **25**, 543–546.
- England, P., Le Fort, P., Molnar, P. & Pecher, A., 1992. Heat sources for tertiary metamorphism and anatexis in the Annapurna-Manaslu region central Nepal. *Journal of Geophysical Research*, **97**, 2107–2128.
- Ferrero, S., Bartoli, O., Cesare, B. *et al.*, 2012. Microstructures of melt inclusions in anatectic metasedimentary rocks. *Journal of Metamorphic Geology*, **30**, 303–322.
- Finch, M., Hasalová, P., Weinberg, R.F. & Fanning, C.M., 2014. Switch from thrusting to extension in the Zaskar Shear Zone, NW Himalaya: structural and metamorphic evidence. *Geological Society of America Bulletin*, **126**, 892–924.
- Gaidies, F., Petley-Ragan, A., Chakraborty, S., Dasgupta, S. & Jones, P., 2015. Constraining the conditions of Barrovian metamorphism in Sikkim, India: P-T-t paths of garnet crystallization in the Lesser Himalayan Belt. *Journal of Metamorphic Geology*, **33**, 23–44.
- Ganguly, J., Dasgupta, S., Cheng, W. & Neogi, S., 2000. Exhumation history of a section of the Sikkim Himalayas, India: records in the metamorphic mineral equilibria and compositional zoning of garnet. *Earth and Planetary Science Letters*, **183**, 471–486.
- Godin, L., Grujic, D., Law, R.D. & Searle, M.P., 2006. Channel flow, ductile extrusion and exhumation in continental collision zones: an introduction. In: *Geological Constraints on Channel Flow and Ductile Extrusion as an Important Orogenic Process – Himalaya-Tibetan Plateau* (eds Law, R.D., Searle, M.P. & Godin, L.), *Geological Society, London, Special Publications*, **268**, 1–23.
- Goscombe, B. & Hand, M., 2000. Contrasting P-T paths in the eastern Himalaya, Nepal: inverted isograds in a paired metamorphic mountain belt. *Journal of Petrology*, **41**, 1673–1719.
- Goscombe, B., Gray, D. & Hand, M., 2006. Crustal architecture of the Himalayan metamorphic front in eastern Nepal. *Gondwana Research*, **10**, 232–255.
- Groppo, C., Rolfo, F., Carosi, R. *et al.*, 2010a. Crustal anatexis in the Higher Himalayan Crystallines of Eastern Nepal: constraints on the P-T evolution of the Barun Gneiss. *Rendiconti Online Società Geologica Italiana*, **11**, 417–418.
- Groppo, C., Rubatto, D., Rolfo, F. & Lombardo, B., 2010b. Early Oligocene partial melting in the Main Central Thrust Zone (Arun valley, eastern Nepal Himalaya). *Lithos*, **118**, 287–301.
- Groppo, C., Rolfo, F. & Indares, A., 2012. Partial melting in the Higher Himalayan crystallines of Eastern Nepal: the effect of decompression and implications for the ‘channel flow’ model. *Journal of Petrology*, **53**, 1057–1088.
- Groppo, C., Rolfo, F. & Mosca, P., 2013. The cordierite-bearing anatectic rocks of the Higher Himalayan crystallines (eastern Nepal): low-pressure anatexis, melt productivity, melt loss and the preservation of cordierite. *Journal of Metamorphic Geology*, **31**, 187–204.

- Grujic, D., Casey, M., Davidson, C. *et al.*, 1996. Ductile extrusion of the Higher Himalayan Crystalline in Bhutan: evidence from quartz microfabrics. *Tectonophysics*, **260**, 21–43.
- Grujic, D., Hollister, L.S. & Parrish, R.R., 2002. Himalayan metamorphic sequence as an orogenic channel: insight from Bhutan. *Earth and Planetary Science Letters*, **198**, 177–191.
- Guillot, S. & Le Fort, P., 1995. Geochemical constraints on the bimodal origin of High Himalayan leucogranites. *Lithos*, **35**, 221–234.
- Guo, Z. & Wilson, M., 2012. The Himalayan leucogranites: constraints on the nature of their crustal source region and geodynamic setting. *Gondwana Research*, **22**, 360–376.
- Harris, N. & Massey, J., 1994. Decompression and anatexis of Himalayan metapelites. *Tectonics*, **13**, 1537–1546.
- Harris, N., Inger, S. & Massey, J., 1993. The role of fluids in the formation of High Himalayan leucogranites. In: *Himalayan Tectonics* (eds Treloar, P.J. & Searle, M.P.), *Geological Society London, Special Publications*, **74**, 391–400.
- Harris, N., Ayres, M. & Massey, J., 1995. Geochemistry of granitic melts produced during the incongruent melting of muscovite: implications for the extraction of Himalayan leucogranite magmas. *Journal of Geophysical Research*, **100**, 15767–15777.
- Harris, N.B.W., Caddick, M., Kosler, J., Goswami, S., Vance, D. & Tindle, A.G., 2004. The pressure-temperature-time path of migmatites from the Sikkim Himalaya. *Journal of Metamorphic Geology*, **22**, 249–264.
- Harrison, T.M., 2006. Did the Himalayan crystallines extrude partially molten from beneath the Tibetan Plateau? In: *Geological Constraints on Channel Flow and Ductile Extrusion as an Important Orogenic Process – Himalaya-Tibetan Plateau* (eds Law, R.D., Searle, M.P. & Godin, L.), *Geological Society, London, Special Publication*, **268**, 237–254.
- Harrison, T.M., Lovera, O.M. & Grove, M., 1997a. New insights into the origin of two contrasting Himalayan granite belts. *Geology*, **25**, 899–902.
- Harrison, T.M., Ryerson, F.J., Le Fort, P., Yin, A., Lovera, O.M. & Catlos, E.J., 1997b. A Late Miocene-Pliocene origin for the Central Himalayan inverted metamorphism. *Earth and Planetary Science Letters*, **146**, E1–E7.
- Harrison, T.M., Grove, M., Lovera, O.M. & Catlos, E.J., 1998. A model of the origin of Himalayan anatexis and inverted metamorphism. *Journal of Geophysical Research*, **103**, 27017–27032.
- Harrison, M.T., Grove, M., McKeegan, K.D., Coath, C.D., Lovera, O.M. & Fort, P.L., 1999a. Origin and episodic emplacement of the Manaslu Intrusive Complex, Central Himalaya. *Journal of Petrology*, **40**, 3–19.
- Harrison, T.M., Grove, M., Lovera, O.M., Catlos, E.J. & D'Andrea, J., 1999b. The origin of Himalayan anatexis and inverted metamorphism: models and constraints. *Journal of Asian Earth Sciences*, **17**, 755–772.
- Hasalová, P., Weinberg, R.F. & MacRae, C., 2013. Microstructural evidence for magma confluence and reusage of magma pathways: implications for magma hybridization, Karakoram Shear Zone in NW India. *Journal of Metamorphic Geology*, **29**, 875–900.
- Herren, E., 1987. Zaskar shear zone: Northeast-southwest extension within the Higher Himalayas (Ladakh, India). *Geology*, **15**, 409–413.
- Hodges, K.V., 1998. The thermodynamics of Himalayan orogenesis. *Geological Society, London, Special Publication*, **138**, 7–22.
- Hodges, K.V., 2000. Tectonics of the Himalaya and southern Tibet from two perspectives. *Geological Society of America Bulletin*, **112**, 324–350.
- Hodges, K.V., Parrish, R.R. & Searle, M.P., 1996. Tectonic evolution of the central Annapurna Range, Nepalese Himalayas. *Tectonics*, **15**, 1264–1291.
- Hodges, K., Bowering, S., Davidek, K., Hawkins, D. & Krol, M., 1998. Evidence for rapid displacement on Himalayan normal faults and the importance of tectonic denudation in the evolution of mountain ranges. *Geology*, **26**, 483–486.
- Horton, F. & Leech, M.L., 2013. Age and origin of granites in the Karakoram shear zone and greater Himalaya sequence, NW India. *Lithosphere*, **5**, 300–320.
- Horton, F., Lee, J., Hacker, B., Bowman-Kamaha'o, M. & Cosca, M., 2015. Himalayan gneiss dome formation in the middle crust and exhumation by normal faulting: new geochronology of Gianbul dome, northwestern India. *Geological Society of America Bulletin*, **127**, 162–180.
- Hubbard, M.S., 1989. Thermobarometric constraints on the thermal history of the Main Central Thrust Zone and Tibetan Slab, eastern Nepal Himalaya. *Journal of Metamorphic Geology*, **7**, 19–30.
- Hubbard, M.S. & Harrison, T.M., 1989.  $^{40}\text{Ar}/^{39}\text{Ar}$  age constraints on deformation and metamorphism in the Main Central Thrust zone and Tibetan Slab, eastern Nepal, Himalaya. *Tectonics*, **8**, 865–880.
- Huerta, A.D., Royden, L.H. & Hodges, K.V., 1996. The interdependence of deformational and thermal processes in mountain belts. *Science*, **273**, 637–639.
- Iaccarino, S., Montomoli, C., Carosi, R., Massonne, H.-J., Langone, A. & Visonà, D., 2015. Pressure-temperature-time-deformation path of kyanite-bearing migmatitic paragneiss in the Kali Gandaki valley (Central Nepal): investigation of Late Eocene-Early Oligocene melting processes. *Lithos*, **231**, 103–121.
- Imayama, T., Takeshita, T., Yi, K. *et al.*, 2012. Two-stage partial melting and contrasting cooling history within the Higher Himalayan Crystalline Sequence in the far-eastern Nepal Himalaya. *Lithos*, **134–135**, 1–22.
- Inger, S. & Harris, N.B.W., 1992. Tectonothermal evolution of the High Himalayan crystalline sequence, Langtang Valley, northern Nepal. *Journal of Metamorphic Geology*, **10**, 439–452.
- Jain, A.K. & Singh, S., 2008. Tectonics of the southern Asian Plate margin along the Karakoram Shear Zone: constraints from field observations and U-Pb SHRIMP ages. *Tectonophysics*, **451**, 186–205.
- Jain, A.K., Shreshtha, M., Seth, P. *et al.*, 2014. The Higher Himalayan Crystallines, Alaknanda – Dhauliganga Valleys, Garhwal Himalaya, India. *Journal of the Virtual Explorer*, **47**, paper 8.
- Jamieson, R.A., Beaumont, C., Medvedev, S. & Nguyen, M.H., 2004. Crustal channel flows: 2. Numerical models with implications for metamorphism in the Himalayan-Tibetan orogen. *Journal of Geophysical Research B: Solid Earth*, **109**(B06407), 1–24.
- Jaupart, C. & Provost, A., 1985. Heat focussing, granite genesis and inverted metamorphic gradients in continental collision zones. *Earth and Planetary Science Letters*, **73**, 385–397.
- Jessup, M.J., Cottle, J.M., Searle, M.P. *et al.*, 2008. P-T-t-D paths of Everest series schist, Nepal. *Journal of Metamorphic Geology*, **26**, 717–739.
- Kellett, D.A. & Grujic, D., 2012. New insight into the South Tibetan detachment system: not a single progressive deformation. *Tectonics*, **31**, TC2007.
- Kellett, D.A., Grujic, D. & Erdmann, S., 2009. Miocene structural reorganization of the South Tibetan detachment, eastern Himalaya: implications for continental collision. *Lithosphere*, **1**, 259–281.
- Kellett, D.A., Grujic, D., Coutand, I., Cottle, J. & Mukul, M., 2013. The South Tibetan detachment system facilitates ultra rapid cooling of granulite-facies rocks in Sikkim Himalaya. *Tectonics*, **32**, 252–270.
- Kelsey, D.E., Clark, C. & Hand, M., 2008. Thermobarometric modelling of zircon and monazite growth in melt-bearing systems: examples using model metapelitic and metapsammitic granulites. *Journal of Metamorphic Geology*, **26**, 199–212.
- King, J., Harris, N., Argles, T., Parrish, R. & Zhang, H., 2011. Contribution of crustal anatexis to the tectonic evolution of

- Indian crust beneath Southern Tibet. *Geological Society of America Bulletin*, **123**, 218–239.
- Klemperer, S.L., Kennedy, B.M., Sastry, S.R., Makovsky, Y., Harinarayana, T. & Leech, M.L., 2013. Mantle fluids in the Karakoram fault: helium isotope evidence. *Earth and Planetary Science Letters*, **366**, 59–70.
- Knesel, K.M. & Davidson, J.P., 2002. Insights into collisional magmatism from isotopic fingerprints of melting reactions. *Science*, **296**, 2206–2208.
- Kohn, M.J., 2008. P-T-t data from central Nepal support critical taper and repudiate large-scale channel flow of the Greater Himalayan sequence. *Geological Society of America Bulletin*, **120**, 259–273.
- Kohn, M.J., 2014. Himalayan metamorphism and its tectonic implications. *Annual Review of Earth and Planetary Sciences*, **42**, 381–419.
- Kohn, M.J., Wieland, M.S., Parkinson, C.D. & Upreti, B.N., 2004. Miocene faulting at plate tectonic velocity in the Himalaya of central Nepal. *Earth and Planetary Science Letters*, **228**, 299–310.
- Kohn, M.J., Wieland, M.S., Parkinson, C.D. & Upreti, B.N., 2005. Five generations of monazite in Langtang gneisses: implications for chronology of the Himalayan metamorphic core. *Journal of Metamorphic Geology*, **23**, 399–406.
- Kohn, M.J., Corrie, S.L. & Markley, C., 2015. The fall and rise of metamorphic zircon. *American Mineralogist*, **100**, 897–908.
- Lacassin, R., Valli, F., Arnaud, N. *et al.*, 2004. Large-scale geometry, offset and kinematic evolution of the Karakoram fault, Tibet. *Earth and Planetary Science Letters*, **219**, 255–269.
- Langille, J.M., Jessup, M.J., Cottle, J.M., Lederer, G. & Ahmad, T., 2012. Timing of metamorphism, melting and exhumation of the Leo Pargil dome, northwest India. *Journal of Metamorphic Geology*, **30**, 769–791.
- Larson, K.P., Ambrose, T.K., Webb, A.A.G., Cottle, J.M. & Shrestha, S., 2015. Reconciling Himalayan midcrustal discontinuities: the Main Central thrust system. *Earth and Planetary Science Letters*, **429**, 139–146.
- Le Fort, P., 1986. Metamorphism and magmatism during the Himalayan collision. In: *Collision Tectonics* (eds Coward, M.P. & Ries, A.C.), *Geological Society, London, Special Publication No. 19*, 159–172.
- Le Fort, P., Cuney, M., Deniel, C. *et al.*, 1987. Crustal generation of the Himalayan leucogranites. *Tectonophysics*, **134**, 39–57.
- Lederer, G.W., Cottle, J.M., Jessup, M.J., Langille, J.M. & Ahmad, T., 2013. Timescales of partial melting in the Himalayan middle crust: insight from the Leo Pargil dome, northwest India. *Contributions to Mineralogy and Petrology*, **166**, 1415–1441.
- Lee, J. & Whitehouse, M.J., 2007. Onset of mid-crustal extensional flow in southern Tibet: evidence from U/Pb zircon ages. *Geology*, **35**, 45–48.
- Leech, M.L., 2008. Does the Karakoram fault interrupt mid-crustal channel flow in the western Himalaya? *Earth and Planetary Science Letters*, **276**, 314–322.
- Leloup, P.H., Mahéo, G., Arnaud, N. *et al.*, 2010. The South Tibet detachment shear zone in the Dinggye area. Time constraints on extrusion models of the Himalayas. *Earth and Planetary Science Letters*, **292**, 1–16.
- Leloup, P.H., Boutonnet, E., Davis, W.J. & Hattori, K., 2011. Long-lasting intracontinental strike-slip faulting: new evidence from the Karakoram shear zone in the Himalayas. *Terra Nova*, **23**, 92–99.
- Leloup, P.H., Weinberg, R.F., Mukherjee, B.K. *et al.*, 2013. Comment on “Displacement along the Karakoram fault, NW Himalaya, estimated from LA-ICP-MS U-Pb dating of offset geologic markers” published by Shifeng Wang *et al.* in EPSL, 2012. *Earth and Planetary Science Letters*, **363**, 242–245.
- Leloup, P.H., Liu, X., Mahéo, G. *et al.*, 2015. New constraints on the timing of partial melting and deformation along the Nyalam section (Central Himalaya): implications for extrusion models. *Geological Society, London, Special Publication*, **412**, 131–175.
- Mahéo, G., Blichert-Toft, J., Pin, C., Guillot, S. & Pêcher, A., 2009. Partial melting of mantle and crustal sources beneath South Karakoram, Pakistan: implications for the Miocene geodynamic evolution of the India – Asia convergence zone. *Journal of Petrology*, **50**, 427–449.
- Molnar, P., Chen, W.-P. & Padovani, E., 1983. Calculated temperatures in overthrust terrains and possible combinations of heat sources responsible for the Tertiary granites in the greater Himalaya. *Journal of Geophysical Research: Solid Earth*, **88**, 6415–6429.
- Montomoli, C., Iaccarino, S., Carosi, R., Langone, A. & Visonà, D., 2013. Tectonometamorphic discontinuities within the Greater Himalayan Sequence in Western Nepal (Central Himalaya): insights on the exhumation of crystalline rocks. *Tectonophysics*, **608**, 1349–1370.
- Montomoli, C., Carosi, R. & Iaccarino, S., 2015. Tectonometamorphic discontinuities in the Greater Himalayan Sequence: a local or a regional feature? *Geological Society, London, Special Publications*, **412**, 25–41.
- Mottram, C.M., Argles, T.W., Harris, N.B.W. *et al.*, 2014a. Tectonic interleaving along the Main Central Thrust, Sikkim Himalaya. *Journal of the Geological Society*, **171**, 255–268.
- Mottram, C.M., Warren, C.J., Regis, D. *et al.*, 2014b. Developing an inverted Barrovian sequence: insights from monazite petrochronology. *Earth and Planetary Science Letters*, **403**, 418–431.
- Mukul, M., 2010. First-order kinematics of wedge-scale active Himalayan deformation: insights from Darjiling-Sikkim-Tibet (DaSiT) wedge. *Journal of Asian Earth Sciences*, **39**, 645–657.
- Murphy, M.A. & Harrison, T.M., 1999. Relationship between leucogranites and the Qomolangma detachment in the Rongbuk Valley, south Tibet. *Geology*, **27**, 831–834.
- Neogi, S., Dasgupta, S. & Fukuoka, M., 1998. High P-T polymetamorphism, dehydration melting, and generation of migmatites and granites in the Higher Himalayan Crystalline Complex, Sikkim, India. *Journal of Petrology*, **39**, 61–99.
- Noble, S.R. & Searle, M.P., 1995. Age of crustal melting and leucogranite formation from U-Pb zircon and monazite dating in the western Himalaya, Zaskar, India. *Geology*, **23**, 1135–1138.
- Olami, Z., Feder, H.J.S. & Christensen, K., 1992. Self-organized criticality in a continuous, nonconservative cellular automaton modeling earthquakes. *Physical Review Letters*, **68**, 1244–1247.
- Parrish, R.R. & Tirrul, R., 1989. U-Pb age of the Baltoro granite, northwest Himalaya, and implications for monazite U-Pb systematics. *Geology*, **17**, 1076–1079.
- Patiño Douce, A.E. & Harris, N., 1998. Experimental constraints on Himalayan Anatexis. *Journal of Petrology*, **39**, 689–710.
- Pêcher, A., 1989. The metamorphism in the Central Himalaya. *Journal of Metamorphic Geology*, **7**, 31–41.
- Phillips, R.J., 2008. Geological map of the Karakoram fault zone, Eastern Karakoram, Ladakh, NW Himalaya. *Journal of Maps*, **4**, 21–37.
- Phillips, R.J., Parrish, R.R. & Searle, M.P., 2004. Age constraints on ductile deformation and long-term slip rates along the Karakoram fault zone, Ladakh. *Earth and Planetary Science Letters*, **226**, 305–319.
- Pognante, U., 1992. Migmatites and leucogranites of tertiary age from the High Himalayan Crystallines of Zaskar (NW India): a case history of anatexis of Paleozoic orthogneisses. *Mineralogy and Petrology*, **46**, 291–313.
- Pognante, U. & Benna, P., 1993. Metamorphic zonation, migmatization and leucogranites along the Everest transect of Eastern Nepal and Tibet: record of an exhumation history. *Geological Society London, Special Publication*, **74**, 323–340.

- Pognante, U. & Lombardo, B., 1989. Metamorphic evolution of the High Himalayan crystallines in SE Zaskar, India. *Journal of Metamorphic Geology*, **7**, 9–17.
- Prince, C., Harris, N. & Vance, D., 2001. Fluid-enhanced melting during prograde metamorphism. *Journal of the Geological Society*, **158**, 233–242.
- Ravikant, V., 2006. Utility of Rb-Sr geochronology in constraining Miocene and Cretaceous events in the eastern Karakoram, Ladakh, India. *Journal of Asian Earth Sciences*, **27**, 534–543.
- Ravikant, V., Wu, F.Y. & Ji, W.Q., 2009. Zircon U-Pb and Hf isotopic constraints on petrogenesis of the Cretaceous-Tertiary granites in eastern Karakoram and Ladakh, India. *Lithos*, **110**, 153–166.
- Reichardt, H. & Weinberg, R.F., 2012a. The dike swarm of the Karakoram shear zone, Ladakh, NW India: linking granite source to batholith. *Geological Society of America Bulletin*, **124**, 89–103.
- Reichardt, H. & Weinberg, R.F., 2012b. Hornblende chemistry in meta- and diatexites and its retention in the source of leucogranites: an example from the Karakoram shear Zone, NW India. *Journal of Petrology*, **53**, 1287–1318.
- Reichardt, H., Weinberg, R.F., Andersson, U.B. & Fanning, M.C., 2010. Hybridization of granitic magmas in the source: the origin of the Karakoram Batholith, Ladakh, NW India. *Lithos*, **116**, 249–272.
- Robyr, M., Hacker, B.R. & Mattinson, J.M., 2006. Doming in compressional orogenic settings: new geochronological constraints from the NW Himalaya. *Tectonics*, **25**, TC2007.
- Robyr, M., Epard, J.L. & El Korh, A., 2014. Structural, metamorphic and geochronological relations between the Zaskar Shear Zone and the Miyar Shear Zone (NW Indian Himalaya): evidence for two distinct tectonic structures and implications for the evolution of the High Himalayan Crystalline of Zaskar. *Journal of Asian Earth Sciences*, **79**, 1–15.
- Rolland, Y. & Pêcher, A., 2001. The Pangong granulites of the Karakoram Fault (Western Tibet): vertical extrusion within a lithosphere-scale fault? *Comptes Rendus de L'Academie des Sciences, Serie II, Fascicule A – Sciences de la Terre et des Planetes*, **332**, 363–370.
- Rubatto, D., Chakraborty, S. & Dasgupta, S., 2013. Timescales of crustal melting in the Higher Himalayan crystallines (Sikkim, Eastern Himalaya) inferred from trace element-constrained monazite and zircon chronology. *Contributions to Mineralogy and Petrology*, **165**, 349–372.
- Sachan, H.K., Kohn, M.J., Saxena, A. & Corrie, S.L., 2010. The Malari leucogranite, Garhwal Himalaya, northern India: chemistry, age, and tectonic implications. *Geological Society of America Bulletin*, **122**, 1865–1876.
- Scaillot, B., France-Lanord, C. & Le Fort, P., 1990. Badrinath-Gangotri plutons (Garhwal, India): petrological and geochemical evidence for fractionation processes in a high Himalayan leucogranite. *Journal of Volcanology and Geothermal Research*, **44**, 163–188.
- Scaillot, B., Pêcher, A., Rochette, P. & Champenois, M., 1995a. The Gangotri granite (Garhwal Himalaya): laccolithic emplacement in an extending collisional belt. *Journal of Geophysical Research*, **100**, 585–607.
- Scaillot, B., Pichavant, M. & Roux, J., 1995b. Experimental crystallization of leucogranite magmas. *Journal of Petrology*, **36**, 663–705.
- Scaillot, B., Holtz, F., Pichavant, M. & Schmidt, M., 1996. Viscosity of Himalayan leucogranites: implications for mechanisms of granitic magma ascent. *Journal of Geophysical Research*, **101**, 27691–27699.
- Schärer, U., Copeland, P., Harrison, T.M. & Searle, M.P., 1990. Age, cooling history, and origin of post-collisional leucogranites in the Karakoram batholith: a multi-system isotope study. *Journal of Geology*, **98**, 233–251.
- Searle, M., 2013. Crustal melting, ductile flow, and deformation in mountain belts: cause and effect relationships. *Lithosphere*, **5**, 547–554.
- Searle, M.P., Weinberg, R.F. & Dunlap, W.J., 1998. Transpressional tectonics along the Karakoram fault zone, northern Ladakh: constraints on Tibetan extrusion. *Continental Transpressional and Transpressional Tectonics*, **135**, 307–326.
- Searle, M.P., Law, R.D. & Jessup, M.J., 2006. Crustal structure, restoration and evolution of the Greater Himalaya in Nepal-South Tibet: implications for channel flow and ductile extrusion of the middle crust. In: *Geological Constraints on Channel Flow and Ductile Extrusion as an Important Orogenic Process - Himalaya-Tibetan Plateau* (eds Law, R.D., Searle, M.P. & Godin, L.), vol. 268, pp. 355–378. Geological Society, London, Special Publications.
- Searle, M.P., Parrish, R.R., Thow, A.V., Noble, S.R., Phillips, R.J. & Waters, D.J., 2010. Anatomy, age and evolution of a collisional mountain belt: the Baltoro granite batholith and Karakoram Metamorphic Complex, Pakistani Karakoram. *Journal of the Geological Society, London*, **167**, 183–202.
- Sen, K., Mukherjee, B.K. & Collins, A.S., 2014. Interplay of deformation and magmatism in the Pangong Transpression Zone, eastern Ladakh, India: implications for remobilization of the trans-Himalayan magmatic arc and initiation of the Karakoram Fault. *Journal of Structural Geology*, **62**, 13–24.
- Simpson, R.L., Parrish, R.R., Searle, M.P. & Waters, D.J., 2000. Two episodes of monazite crystallization during metamorphism and crustal melting in the Everest region of the Nepalese Himalaya. *Geology*, **28**, 403–406.
- Sorcar, N., Hoppe, U., Dasgupta, S. & Chakraborty, S., 2014. High-temperature cooling histories of migmatites from the High Himalayan Crystallines in Sikkim, India: rapid cooling unrelated to exhumation? *Contributions to Mineralogy and Petrology*, **167**, 1–34.
- Spear, F.S. & Pyle, J.M., 2010. Theoretical modeling of monazite growth in a low-Ca metapelite. *Chemical Geology*, **273**, 111–119.
- Streule, M.J., Searle, M.P., Waters, D.J. & Horstwood, M.S.A., 2010. Metamorphism, melting, and channel flow in the Greater Himalayan Sequence and Makalu leucogranite: constraints from thermobarometry, metamorphic modeling, and U-Pb geochronology. *Tectonics*, **29**, TC5011.
- Upadhyay, R., 2009. U-Pb zircon age for a granite intrusion within the Shyok suture zone, Saltoro Hills, northern Ladakh. *Current Science*, **97**, 1234–1239.
- Valli, F., Nicolas, A., Leloup, P.H. *et al.*, 2007. Twenty million years of continuous deformation along the Karakoram fault, western Tibet: a thermochronological analysis. *Tectonics*, **26**, TC4004. doi: 10.1029/2005TC001913.
- Valli, F., Leloup, P.H., Paquette, J.-L. *et al.*, 2008. New U-Th/Pb constraints on timing of shearing and long-term slip-rate on the Karakoram fault. *Tectonics*, **27**, TC5007.
- Vance, D. & Harris, N., 1999. Timing of prograde metamorphism in the Zaskar Himalaya. *Geology*, **27**, 395–398.
- Vannay, J.C. & Hodges, K.V., 1996. Tectonometamorphic evolution of the Himalayan metamorphic core between the Annapurna and Dhaulagiri, central Nepal. *Journal of Metamorphic Geology*, **14**, 635–656.
- Viskopic, K. & Hodges, K.V., 2001. Monazite-xenotime thermochronometry: methodology and an example from the Nepalese Himalaya. *Contributions to Mineralogy and Petrology*, **141**, 233–247.
- Viskopic, K., Hodges, K.V. & Bowring, S.A., 2005. Timescales of melt generation and the thermal evolution of the Himalayan metamorphic core, Everest region, eastern Nepal. *Contributions to Mineralogy and Petrology*, **149**, 1–21.
- Visonà, D. & Lombardo, B., 2002. Two-mica and tourmaline leucogranites from the Everest-Makalu region (Nepal - Tibet). Himalayan leucogranite genesis by isobaric heating? *Lithos*, **62**, 125–150.

- Visonà, D., Carosi, R., Montomoli, C., Tiepolo, M. & Peruzzo, L., 2012. Miocene andalusite leucogranite in central-east Himalaya (Everest-Masang Kang area): low-pressure melting during heating. *Lithos*, **144–145**, 194–208.
- Walker, J.D., Martin, M.W., Bowring, S.A., Searle, M.P., Waters, D.J. & Hodges, K.V., 1999. Metamorphism, melting and extension: age constraints from the High Himalayan Slab of southeast Zaskar and northwest Lahaul. *Journal of Geology*, **107**, 473–495.
- Wang, S., Wang, C., Phillips, R.J., Murphy, M.A., Fang, X. & Yue, Y., 2012. Displacement along the Karakoram fault, NW Himalaya, estimated from LA-ICP-MS U-Pb dating of offset geologic markers. *Earth and Planetary Science Letters*, **337–338**, 156–163.
- Weinberg, R.F., 1999. Mesoscale pervasive felsic magma migration: alternatives to dyking. *Lithos*, **46**, 393–410.
- Weinberg, R.F. & Dunlap, W.J., 2000. Growth and deformation of the Ladakh batholith, northwest Himalayas: implications for timing of continental collision and origin of calc-alkaline batholiths. *Journal of Geology*, **108**, 303–320.
- Weinberg, R.F. & Hasalová, P., 2015. Water-fluxed melting of the continental crust: a review. *Lithos*, **212–215**, 158–188.
- Weinberg, R.F. & Mark, G., 2008. Magma migration, folding, and disaggregation of migmatites in the Karakoram Shear Zone, Ladakh, NW India. *Geological Society of America Bulletin*, **120**, 994–1009.
- Weinberg, R.F. & Regenauer-Lieb, K., 2010. Ductile fractures and magma migration from source. *Geology*, **38**, 363–366.
- Weinberg, R.F. & Searle, M.P., 1998. The Pangong Injection Complex, Indian Karakoram: a case of pervasive granite flow through hot viscous crust. *Journal of the Geological Society*, **155**, 883–891.
- Weinberg, R.F. & Searle, M.P., 1999. Volatile-assisted intrusion and autometasomatism of leucogranites in the Khumbu Himalaya, Nepal. *Journal of Geology*, **107**, 27–48.
- Weinberg, R.F., Mark, G. & Reichardt, H., 2009. Magma ponding in the Karakoram shear zone, Ladakh, NW India. *Geological Society of America Bulletin*, **121**, 278–285.
- Yakymchuk, C. & Brown, M., 2014. Behaviour of zircon and monazite during crustal melting. *Journal of the Geological Society*, **171**, 465–479.
- Yin, A. & Harrison, T.M., 2000. Geologic evolution of the Himalayan-Tibetan orogen. *Annual Review of Earth and Planetary Sciences*, **28**, 211–280.
- Zeiger, K., Gordon, S.M., Long, S.P., Kylander-Clark, A.R.C., Agustsson, K. & Penfold, M., 2015. Timing and conditions of metamorphism and melt crystallization in Greater Himalayan rocks, eastern and central Bhutan: insight from U-Pb zircon and monazite geochronology and trace-element analyses. *Contributions to Mineralogy and Petrology*, **169**, 19.
- Zhang, H., Harris, N., Parrish, R. *et al.*, 2004. Causes and consequences of protracted melting of the mid-crust exposed in the North Himalayan antiform. *Earth and Planetary Science Letters*, **228**, 195–212.

Received 6 November 2015; revision accepted 21 May 2016.